Revolutionizing Training-Free NAS: Towards Efficient Automatic Proxy Discovery via Large Language Models

Haidong Kang[1*] **Lihong Lin**[1] **Hanling Wang**[2]
[1]Northeastern University, China [2]Pengcheng Laboratory, China
hdkang@stumail.neu.edu.cn, linlh@mails.neu.edu.cn, wanghl03@pcl.ac.cn

Abstract

The success of computer vision tasks is mainly attributed to the architectural design of neural networks. This highlights the need to automatically design high-performance architectures via Neural Architecture Search (NAS). To accelerate the search process, training-free NAS is proposed, which aims to search high-performance architectures at initialization via zero-cost proxies (ZCPs). However, existing zero-cost proxies heavily rely on manual design, which is often labor-intensive and requires extensive expert knowledge. In addition, these crafted proxies often suffer from poor correlation with final model performance and high computational complexity, severely limiting NAS efficiency in real-world applications. To address those issues, this paper proposes a novel Large Language Models (LLMs)-driven Automatic Proxy Discovery (**APD**) framework, which revolutionizes the design paradigm of ZCPs by leveraging LLMs to automatically discover optimal ZCPs for Training-Free NAS. Moreover, we utilize actor-critic based reinforcement learning to optimize prompts, enabling to generate better ZCPs in the next generation. We conduct extensive experiments on mainstream NAS benchmarks, demonstrating APD excels in both performance and efficiency. Besides, we firmly believe that our APD will dramatically benefit the deep learning community through providing novel paradigm of design algorithms via LLMs.

1 Introduction

Neural networks plays an indispensable role in computer vision tasks due to its superior performance, which raises a trend to deploy neural networks (i.e., ResNet He et al. [2016]) on resource-intensive scenarios. However, conventional neural networks designed by human experts suffer from Out-Of-Memory (OOM) problems due to dramatically limited resources Xie et al. [2023], Kang et al. [2025]. Therefore, this highlights the need to design lightweight architectures, liberating the handicraft neural networks from the OOM bottleneck.

Recently, Neural Architecture Search (NAS) Liu et al. [2018], Ye et al. [2022], Kang has emerged as a promising paradigm for its searching high-performance architectures in an automatic manner, while disrupting the conventional paradigm of manually designed architecture. Despite its potential, NAS still suffers from a key bottleneck of huge computational budgets Ma et al. [2024]. To tackle this, training-free NAS Mellor et al. [2021], Abdelfattah et al. [2021], Wang et al. [2020], Chen et al. [2022], Lee and Ham [2024], Peng et al. [2024] is proposed to liberate NAS from the computational bottleneck via the lens of without gradient descent. Essentially, the training-free NAS leverages ZCPs, predicting the accuracy ranking of architectures in a training-free manner. Specifically, the ZCPs rely

*Corresponding author

Preprint. Under review.

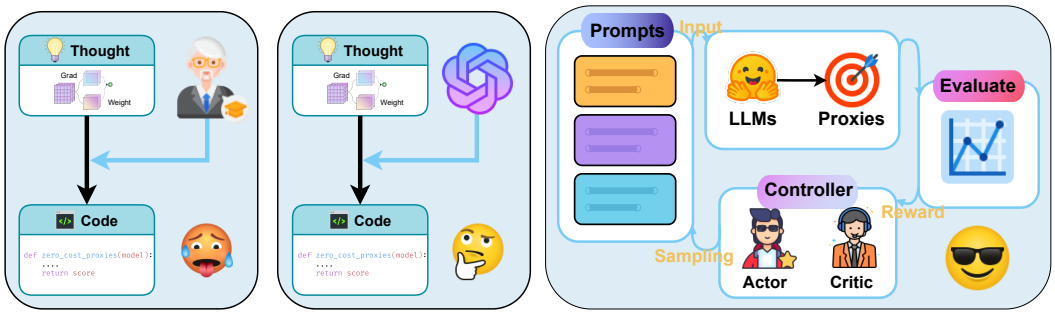

(a) Manual Design (b) Naive method (c) Ours

Figure 1: A comparison of the designed way of ZCPs. (a) Manual design relies on expert knowledge. (b) A naive method via LLMs. (c) Our method proposes an LLM-driven APD framework to automatically discover optimal ZCPs for Training-Free NAS.

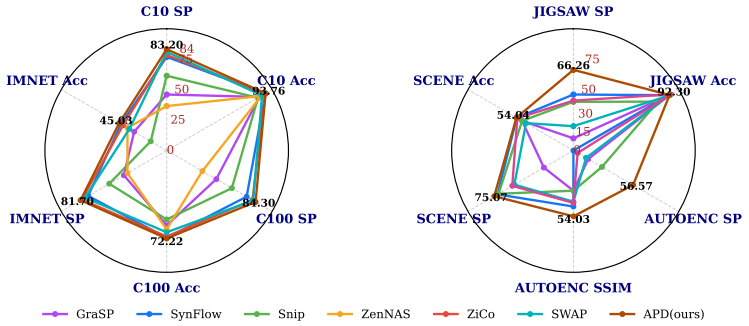

Figure 2: Spearman (SP) ranking correlations & accuracies (Acc) of zero-cost proxies on NAS-Bench-201 (Left) and Trans-Bench-101 (right).

on some statistical or theoretical properties (i.e., the number of parameters, Neural Tangent Kernel) of neural architectures to assess their expressivity.

1.1 Challenges

Although these approaches have taken the first step towards ZCPs tailored for training-free NAS Haidong et al. [2025], current ZCPs still suffer from several fatal drawbacks: (1) *they require extensive expert knowledge through hundreds of time-consuming trial-and-error processes (as shown in Fig. 1a and Table 1), increasing the labor costs and making it hard to design new ZCPs; (2) these crafted ZCPs incur poor correlation with the final accuracy of searched architecture (as shown in Fig. 2 and 3), making the users do not know why those ZCPs failed and hard to deploy in real-world applications.* This is identified with ZiCO Li et al. [2023], which points out that the performance of simple proxies (i.e., #Params, FLOPs) excels most of the crafted ZCPs. Those limitations highlight the need to rethink the design paradigm of AZPs.

Our New Observation. Different from existing methods for training-free NAS, as depicted in Fig. 1b, and Fig. 1c, we observe a new way to automatically design ZCPs via Large Language Models (LLMs) in this work, which can effectively address the aforementioned drawbacks by revolutionizing the traditional manual design manner. More details are shown in Section 3.

1.2 Contributions

In this work, we attempt to analyze and address the above drawbacks. To fulfill our goal, we first conduct an in-depth analysis by rethinking the design of ZCPs, and experimentally confirm their limitations (as shown in Section 2). To tackle those drawbacks, motivated by powerful large language models (LLMs) Radford et al. [2018], Brown et al. [2020], Achiam et al. [2023], Chang et al. [2024], Liu et al. [2024] for generating new ideas and knowledge, we provide an affirmative answer by proposing a novel way to automatically design ZCPs via LLMs, dubbed APD. Specifically, we first explore a naive method (as depicted in Fig. 1b) using a simple prompt as input to LLMs, however,

Spearman (SP) ranking correlation of ZCPs searched by the naive method is very poor. This raises the challenge and need of how to seek new strategy, improving the effectiveness of LLM-driven ZCPs. To reveal the root cause, we conduct an in-depth analysis and observe that the naive method lacks thought between the prompt and tasks, which could be a potential reason of poor correlation. Inspired by GPT-4o and Deepseek R1 Guo et al. [2025], we leverage actor-critic based reinforcement learning (as shown in Fig. 1c) as the reasoning engine, enabling it to generate intermediate reasoning steps before the final answer. This plays a critical Chain-of-Thought (CoT) role in enhancing APD performance, especially in NAS tasks requiring multi-step reasoning. We summarize the main contributions of this work as follows:

- **New ZCPs paradigm.** To the best of our knowledge, we are the first to propose a novel ZCPs paradigm by leveraging LLMs, providing a new perspective for understanding and designing training-free NAS.
- **CoT driven strategy**. Beyond the limit of poor correlation of simple prompts for designing ZCPs, we first reveal that the root cause is the absence of positive reward signals for these proxies during search. To address this, we propose an actor-critic based reinforcement learning to build reasoning engine, achieving improvements akin to Chain-of-Thought reasoning in GPT-4o and DeepSeek-R1 and yielding much stronger proxy-to-performance correlation.
- **Numerical Verification.** Extensive experiments validate the superiority of our APD, outperforming previous methods on mainstream search spaces and datasets.

2 Rethinking the design of Zero-cost Proxies

The primary goal of AZPs is to accurately predict the ranking of architectures without training on a given search space. As shown in Table 1, the representative AZPs (i.e., SNIP, SWAP) leverage heuristics, statistical, or gradient properties to measure expressibility of architectures. However, those AZPs heavily rely on human expertise, which may be suboptimal for new search spaces or datasets. In addition, designing new ZCPs is time-consuming.

Method	Corresponding formula	Human expert
SNIP	$\left\lvert\left(\frac{\partial \mathcal{L}}{\partial \theta}\right) \odot \theta\right\rvert$	✓
Fisher	$\sum_{z \in A}\left(\frac{\partial \mathcal{L}}{\partial z} z\right)^2$	✓
SynFlow	$\left(\frac{\partial \mathcal{R}}{\partial \theta}\right) \odot \theta, \mathcal{R}=\mathbb{1}^T\left(\prod_{\theta_i \in W}\lvert\theta_i\rvert\right) \mathbb{1}$	✓
AZ-NAS	$s^{\mathrm{AZ}}(i)=\sum_{\mathcal{M} \in\{\mathcal{E}, \mathcal{P}, \mathcal{T}, \mathcal{C}\}} \log \frac{\operatorname{Rank}\left(s^{\mathcal{M}}(i)\right)}{m}$	✓
SWAP	$\Psi_{\mathcal{N}, \theta}=\left\lvert\hat{\mathbb{A}}_{\mathcal{N}, \theta}\right\rvert$	✓
APD	$s^{\mathrm{APD}}=\left(\sum_{l \in \mathcal{B}} \frac{\lVert M_l(\theta)\rVert_F^2}{\lVert M_l(\theta)\rVert_2^2}\right) \times\left(\sum_{l \in \mathcal{C}} \frac{\lVert W_l(\theta)\rVert_1}{\lVert W_l(\theta)\rVert_2}\right)$	✗

Table 1: Comparison of existing ZCPs. Here, s^{APD} is the best-performing ZCP discovered by APD on NAS-Bench-201. In APD, $\mathcal{B}$ and $\mathcal{C}$ represent batchnorm and convolutional layers, while M and W denote their outputs and weights.

Notably, ZiCO Li et al. [2023] highlights that simple proxies such as the number of parameters and FLOPs often outperform many hand-crafted ZCPs in predicting neural architecture performance. As shown in Fig. 3, hand-crafted ZCPs (i.e., Grasp, AZ-NAS, SWAP) suffer from a significant poor correlation issue. Those experimentation with hand-crafted ZCPs motivate us to seek a new ZCPs paradigm for designing training-free NAS.

Inspired by the knowledge generation capabilities of LLMs, we raise a new question: can LLMs automatically generate zero-cost proxies (ZCPs) for NAS tasks? To test this, we designed a simple prompt (**App. A**) that asks the LLM to output a ZCP, based on the assumption that LLMs have internalized rich knowledge of neural networks during pretraining. On NAS-Bench-201, the generated ZCP achieved a 60.51% spearman correlation (as shown in Table 7) on NAS-Bench-201 search space in CIFAR-10 dataset, lower than hand-crafted methods, yet encouraging for LLM-driven ZCP discovery. Further analysis reveals that the lack of reasoning and feedback is the key limitation, as prompt-based generation is a black-box process. To address this, we propose an actor–critic reinforcement learning framework, inspired by Chain-of-Thought (CoT) prompting in GPT-4o. This

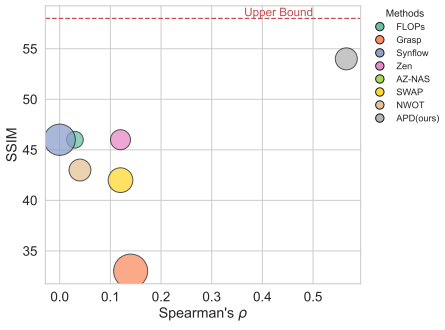

Figure 3: A comparison of ZCPs on AutoEncoding of Trans-Bench-101.

design introduces a feedback loop between the LLM
and the NAS task, enabling the LLM to refine ZCPs iteratively and significantly improving both the performance and efficiency of proxy generation (as shown in Fig. 3).

3 APD: A Resourceful Adviser for Training-Free NAS

3.1 Automatic Proxy Discovery

To fulfill the goal of designing ZCPs for the training-free NAS, APD utilizes LLMs to automatically generate proxies by evolving both natural language descriptions and corresponding code. In addition, we propose an actor-critic RL controller sampling appropriate prompt strategies to guide the evolution, aiming to optimize the correlation between proxies and final model performance. The overall framework of APD is depicted in Fig. 4, which consisting of three main components as follows:

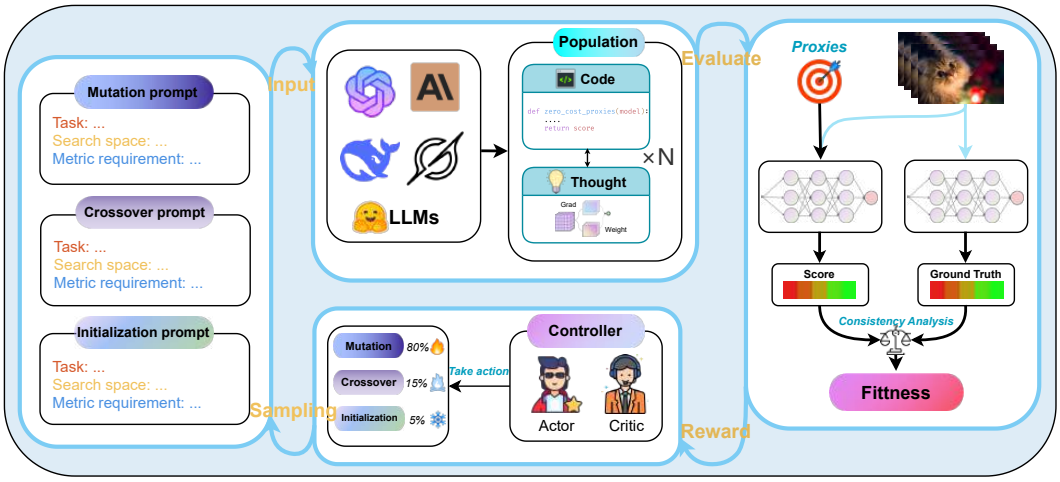

Figure 4: Overview of APD. APD utilizes large-scale pre-trained models to automatically search for the optimal zero-cost proxies tailored for training-free NAS.

Proxy Candidate Generator. LLM in APD serves as proxy candidate generator. Carefully structured prompts enable it to synthesize new ZCPs or refine existing ZCPs. Let $\mathcal{P}$ denote the set of valid proxies that satisfy a fixed I/O contract. During time step t, with the current proxy population $P_t (P_t \subseteq \mathcal{P})$, the LLM $\mathcal{L}$ receives both a structured prompt $\pi \in \Pi$ that specifies the requested operation $\Pi(\text{initialization}, \text{mutation}, \text{crossover})$ and a bounded context window $\mathcal{C}_t \subseteq P_t$ containing existing proxies together with their natural language rationales and codes. This pair $(\pi, \mathcal{C}_t)$ induces a context-conditioned distribution:

$$\mu_{\pi,\mathcal{C}_t} = \mathrm{P}_{\mathcal{L}}(f|\pi, \mathcal{C}_t), \tag{2}$$

where $\mu_{\pi,\mathcal{C}_t}$ represents the probability distribution over candidate proxies induced by prompt π and context $\mathcal{C}_t$ with LLM $\mathcal{L}$. Composing over all prompts and admissible contexts yields an implicit, context-aware search space:

$$\mathcal{F} = \bigcup_{t \in N} \bigcup_{\pi \in \Pi} \bigcup_{\mathcal{C} \subseteq P_t} \mathrm{supp}(\mu_{\pi,\mathcal{C}}), \tag{3}$$

where $\mathrm{supp}(\mu_{\pi,\mathcal{C}})$ is the support set of distribution $\mu_{\pi,\mathcal{C}}$. Obviously, we have $\mathcal{F} \subseteq \mathcal{P}$. Relative to context-free pairs, this construction enlarges support while preserving ergodic reachability and allows the generator to reuse salient patterns already discovered in $\mathcal{P}$, and thereby drives the realized search space $\mathcal{A}$ to lie as close as possible to $\mathcal{P}$.

In APD, three categories of context-conditioned pairs are employed, each of which gives rise to distinct distribution:

- **Initialization** $\mu_{\text{init},\emptyset}$ provides only the task description, I/O contract and ample prior knowledge that depicts input architectures and data.

- **Mutation** $\mu_{\mathrm{mut},f}$ conditions on a single proxy f to perform local perturbations, enabling fine-grained exploitation.
- **Crossover** $\mu_{\mathrm{cross},\mathbf{f}}$ furnishes at least two parent proxies and asks the LLM to identify their common principles and fuse complementary components, encouraging recombination of useful motifs.

The context-aware Proxy Candidate Generator endows APD with flexible exploration granularity: during a single evolutionary step, the algorithm can elect either to densely sample previously unvisited regions of the proxy space or to perform fine-grained, local refinement around promising candidates, thus supporting both broad coverage and deep exploitation as needed.

Fitness Evaluator. The fitness evaluator swiftly quantifies each candidates ZCP by computing its Spearman correlation with ground-truth accuracies on the given NAS benchmark $\mathcal{A}$ (e.g., NAS-Bench-201). For a benchmark set $\mathcal{B} = \{(a_i, p_i)\}_{i=1}^{m}$ of architectures and ground-truth accuracies under dataset $\mathcal{D}$. The fitness assigned to f is

$$\phi(f) = \rho(f(\mathbf{a}), \mathbf{p}) - \beta \mathrm{cost}(f). \tag{4}$$

Where ρ is Spearman or Kendall correlation, computed on randomly sampled subset of $\mathcal{B}$ to provide an unbiased estimate of ranking fidelity. $\mathrm{cost}(f)$ is the average runtime required to evaluate one architecture of $\mathcal{B}$. β is a hyperparameter that controls the trade-off between predictive quality and computational efficiency.

RL Evolution Scheduler. To render the proxy evolution strategy learnable and capable of converging efficiently toward optimal ZCPs, APD introduces an actor–critic module that serves as the evolutionary decision-maker. The actor–critic treats the fitness score returned by the evaluator as its reward and learns a policy that maximizes this signal, thereby jointly optimizing both the evolving set of ZCPs and the evolution strategy itself.

In a given search space $\mathcal{A}$ of candidate architectures and their ground-truth performance $p(a)$, the objective of APD is to learn a proxy $f : \mathcal{A} \to \mathbb{R}$ whose scores preserve the ranking induced by p. Therefore, we aim to maximize the expected correlation:

$$\max_{f \in \mathcal{F}} \mathbb{E}_{\mathbf{a} \subseteq \mathcal{A}}[\rho(f(\mathbf{a}), p(\mathbf{a}))], \tag{1}$$

where ρ is Spearman ρ_s. Each proxy f is represented as a tuple $(\mathcal{T}, \mathcal{C})$ of $\mathcal{T}$ a natural language thought describing the proxy's principle, and $\mathcal{C}$ an executable code that returns a scalar score, ensuring interpretability and deterministic replay throughout the evolutionary process.

To accelerate convergence toward high correlation proxies while maintaining effective exploration in search space $\mathcal{F}$, APD introduces a light-weight Actor-Critic as evolution scheduler that governs every evolutionary step. At generation t, the controller observes a compact state vector with fixed-width histogram of fitness values and strategies, sampling an action $a_t \in \Pi$ from a categorical policy $\pi_\theta(a|s_t)$. Executing a_t yields candidate proxies $P_t^{'}$, whose fitness $\phi(P_t^{'})$ is evaluated by the Fitness Evaluator. The scheduler then receives a clipped reward $r_t = \mathbb{E}(\phi(P_t^{'}))$ that promotes substantive improvements and updates the Actor-Critic by standard advantage-actor-critic gradient steps:

$$\begin{aligned} \theta \leftarrow & \theta + \eta \nabla_\theta \log \pi_\theta(a_t \mid s_t) \left[r_t + \gamma V_\psi(s_{t+1}) - V_\psi(s_t) \right], \\ \psi \leftarrow & \psi - \eta_v \nabla_\psi \big(r_t + \gamma V_\psi(s_{t+1}) - V_\psi(s_t) \big)^2. \end{aligned} \tag{5}$$

Where θ and ψ denote the actor and critic parameters, η and η_v are the actor and critic learning rates, V_ψ is the value baseline parameterized by ψ, and γ is the discount factor. The critic minimizes $(r + \gamma V(s_{t+1}) - V(s_t))^2$, and the actor maximizes the advantage-weighted log likelihood.

3.2 Evolution Framework

Based on the components outlined in Section 3.1, we integrate the Proxy Candidate Generator, Fitness Evaluator, and the RL Evolution Scheduler into evolutionary loop. As shown in **Algorithm** 1, APD unfolds through the following mutually dependent steps:

Step 0 Initialization In time step 0, an $(\mathrm{initialization}, \emptyset)$ is issued to the LLM, producing the seed $P_0 = \{f_1, \cdots, f_N\}$.

Step 1 Generation At generation t the actor samples an action $a_t = (\mathrm{op}, C_t) \sim \pi_\theta(\cdot|s_t)$ where $\mathrm{op} \in \{\mathrm{init}, \mathrm{mut}, \mathrm{cross}\}$. The corresponding prompt and context window $\mathcal{C}_t \subseteq P_t$ are fed to the LLM, yielding candidate proxies $P_t^{'}$.

Step 2 Evaluation The candidates are scored in $\mathcal{B}$ by the fitness function $\phi(\cdot)$. If the proxy fails the contract check, it is assigned $\phi = -\infty$.

Step 3 Policy update The scheduler receives reward $r_t = \mathbb{E}(\phi(f))$ by calculating the mean ϕ and updates (θ, ψ) by the rule in (5).

Step 4 Population replacement The union $P_t \cup \{P_t^{'}\}$ is sorted by fitness. The worst proxies are dropped to keep $|P_{t+1}| = N$. A tie-breaking rule that favors younger proxies prevents age-related stagnation. The loop then returns to **Step 1**.

The loop terminates after T_{max} generations. Empirically, the framework produced proxies whose Spearman correlation on NASBench201 exceeds 0.80 within 30 generations roughly one GPU-hour on a single RTX4090.

Algorithm 1 Evolution Framework

Require: LLM $\mathcal{L}$, benchmark $\mathcal{B}$, population N, budget T_{max}, actor-critic (π_θ, V_ψ)
  $P_0 \leftarrow$ first N proxies from $\mu_{\mathrm{init},\emptyset}$, $s_0 \leftarrow \{\emptyset, \emptyset\}$
  for $t = 1$ to T_{max} **do**
    $\mathrm{op} \sim \pi(\cdot|s_t)$, $\mathcal{C} \leftarrow P$
    $P^{'} \leftarrow \mathcal{L}(\mu_{\mathrm{op},\mathcal{C}})$, $\varphi \leftarrow \phi(P^{'})$
    $r_t \leftarrow \mathbb{E}(\varphi)$, update (θ, ψ, s_{t+1})
    $P \leftarrow (P \cup P^{'})/\{\mathrm{worst}(P)\}$
  end for
  return $\arg\max_{f \in \mathcal{F}} \phi(f)$

4 Experiments

4.1 Experimental Settings

We evaluate APD on 5 representative search spaces (e.g., NAS-Bench-201 Dong and Yang [2020], NAS-Bench-101 Ying et al. [2019], DARTS Liu et al. [2018], TransNAS-Bench-101–Micro Duan et al. [2021], OoD-ViT-NAS Bai et al. [2021]) across 4 tasks: image recognition, autoencoding, scene classification, and self-supervised jigsaw puzzles. We transfer the zero-cost proxy identified on CIFAR-10 within the NAS-Bench-201 search space to all datasets in both NAS-Bench-201 and NAS-Bench-101. However, due to the substantial search space disparities between TransNAS-Bench-101, OoD-ViT-NAS, and NAS-Bench-201, we search for new zero-cost proxies directly within these spaces to ensure optimal performance. In addition, we train APD with 7 mainstream LLMs (i.e., GPT4o Achiam et al. [2023], Claude 3.7 Anthropic [2025], Deepseek V3 Liu et al. [2024], Gemini flash Google Cloud [2025], Llama 4 Meta AI [2025], Grok 3 xAI [2025]). Full experimental details are provided in **App. B**.

4.2 Performance on NAS-Bench-201&101 search spaces

Table 5 compares APD with state-of-the-art training-free NAS methods on NAS-Bench-201 (CIFAR-10/100, ImageNet16-120) and NAS-Bench-101 (CIFAR-10). APD consistently achieves the highest test accuracy and ranking correlations (SPR/KT) across all datasets. Compared to the best existing methods, APD improves test accuracy by +0.07% on CIFAR-10 (vs. ZiCo), +0.52% on CIFAR-100 (vs. Synflow), and +0.69% on ImageNet16-120 (vs. AZ-NAS), while reducing runtime cost by over 50%. On ImageNet16-120, APD also outperforms Grasp by +14.18%, ZenNAS by +7.85%, ZiCo by +3.61%, and AZ-NAS by +0.69%. These results not only highlight the efficiency and robustness of APD across diverse search spaces, but also demonstrate the strong potential of LLM-driven ZCP design, advancing the development of training-free NAS.

Table 2: Performance comparison on NAS-Bench-201 (NB-201) search space with CIFAR-10/100, and ImageNet16-120 datasets, and NAS-Bench-101 (NB-101) search space with CIFAR-10 dataset. We report Kendall's τ (KT) and Spearman's ρ (SPR) computed with all candidate architectures. In addition, we report the average independent runs results obtained from our method. The red, blue, and orange indicate the best, second-best, and third-best results, respectively.

Method	CIFAR-10(NB-201)			CIFAR-100(NB-201)			ImageNet16-120(NB-201)			CIFAR10(NB-101)		Runtime (ms/arch)
	SPR	KT	Test acc.(%)	SPR	KT	Test acc.(%)	SPR	KT	Test acc.(%)	SPR	Test acc.(%)	
Params	0.751	0.576	93.61 ± 0.08	0.726	0.552	70.95 ± 0.37	0.690	0.519	41.67 ± 0.64	0.38	92.18 ± 1.53	-
FLOPs	0.733	0.541	93.61 ± 0.08	0.708	0.517	70.95 ± 0.37	0.691	0.517	41.67 ± 0.64	0.67	92.18 ± 1.53	-
Snip Abdelfattah et al. [2021]	0.614	0.455	86.63 ± 3.89	0.618	0.461	56.53 ± 7.56	0.545	0.409	15.13 ± 10.86	0.71	85.41 ± 1.38	45.78
Grasp Abdelfattah et al. [2021]	0.460	0.318	88.01 ± 3.14	0.470	0.329	61.43 ± 7.04	0.406	0.282	30.85 ± 5.66	0.45	87.08 ± 1.40	93.70
Synflow Abdelfattah et al. [2021]	0.769	0.571	93.67 ± 0.39	0.758	0.562	71.70 ± 0.94	0.745	0.553	43.39 ± 3.21	0.38	89.93 ± 2.97	78.26
NWOT Mellor et al. [2021]	0.743	0.557	91.95 ± 1.29	0.769	0.579	68.88 ± 1.60	0.760	0.573	42.31 ± 3.43	0.32	93.16 ± 0.36	36.54
ZenNAS Lin et al. [2021]	0.365	0.283	89.55 ± 1.12	0.338	0.245	64.69 ± 3.86	0.372	0.260	37.18 ± 3.17	0.65	93.06 ± 0.73	30.07
ZiCo Li et al. [2023]	0.784	0.589	93.69 ± 0.07	0.813	0.620	70.63 ± 1.08	0.804	0.614	41.42 ± 0.97	0.65	92.64 ± 0.99	75.50
AZ-NAS Lee and Ham [2024]	0.913	0.741	93.49 ± 0.30	0.900	0.723	70.33 ± 1.16	0.886	0.710	44.34 ± 1.26	0.42	92.01 ± 0.85	69.43
SWAP Peng et al. [2024]	0.810	0.634	90.48 ± 0.94	0.820	0.649	67.13 ± 1.83	0.774	0.610	35.40 ± 3.96	0.44	90.51 ± 2.08	47.61
APD	0.832	0.635	93.76 ± 0.09 ↑(0.07)	0.843	0.654	72.22 ± 0.65 ↑(0.52)	0.817	0.633	45.03 ± 0.76 ↑(0.69)	0.73	93.49 ± 0.34 ↑(0.33)	16.81 ↓(13.26)
Optimal	-	-	94.33 ± 0.08	-	-	73.30 ± 0.20	-	-	46.97 ± 0.19	-	93.87 ± 0.08	-

Table 3: Comparison on the DARTS search space using CIFAR-10/100 (left) and ImageNet1k (right). "C10", "C100", and "Img" indicate search conducted on CIFAR-10, CIFAR-100, and ImageNet1k, respectively. All models are retrained using official code from Liu et al. [2018] for fair comparison. "Paper" shows results from original publications; "$*$" denotes results from released training code Zheng et al. [2021]; "–" means unavailable or unreleased data.

Method	CIFAR-10 Top-1 (%)		CIFAR-100 Top-1 (%)	Params (M)	GPU-Days	Search method
	Retrain	Paper	Paper			
ResNet18 He et al. [2016]	-	-	75.61	11.2	-	Manual
AmoebaNet-A Zoph et al. [2018]	-	97.45 ± 0.05	16.82	-	3150	Evolution
ENAS Pham et al. [2018]	-	-	81.09	4.6	0.5	Evolution
PNAS Liu et al. [2018]	-	96.59	82.37	3.2	225	SMBO
NASNet-A Zoph et al. [2018]	-	97.37	82.19	3.3	1,800	RL
DARTS(2nd) Liu et al. [2018]	-	97.24 ± 0.09	82.46	3.3	1	Gradient
DARTS(1nd) Liu et al. [2018]	-	97.00 ± 0.14	83.18	3.3	0.4	Gradient
P-DARTS Chen et al. [2019]	97.30 ± 0.15$*$	97.50	83.37	3.4	0.3	Gradient
PC-DARTS Xu et al. [2019]	97.29 ± 0.11$*$	97.43 ± 0.07	82.89	3.6	0.1	Gradient
DARTS+ Liang et al. [2019]	-	97.50 ± 0.11	83.72	3.7	0.4	Gradient
DARTS- Chu et al. [2020]	97.38$*$	97.41 ± 0.08	82.49	3.5±0.13	0.4	Gradient
FairDARTS-D Chu et al. [2020]	97.29$*$	97.46 ± 0.05	-	3.8	0.4	Gradient
DARTS+PT Wang et al. [2021]	-	97.39 ± 0.08	-	3.0	0.8	Gradient
β-DARTS Ye et al. [2022]	-	97.47 ± 0.08	83.48	3.8±0.15	0.4	Gradient
Λ-DARTS Movahedi et al. [2023]	-	97.48 ± 0.11	83.47	3.5±0.13	-	Gradient
FP-DARTS Wang et al. [2023]	-	97.50 ± 0.05	83.50±0.05	3.9	0.08	Gradient
DARTS-AER^{k} Jing et al. [2023]	-	97.47 ± 0.02	-	3.64 ± 0.18	0.3	Gradient
IS-DARTS He et al. [2024]	-	97.44 ± 0.04	-	4.25 ± 0.22	0.42	Gradient
NWOT Mellor et al. [2021]	95.73	-	-	5.0	-	Training-free
TENAS Chen et al. [2021]	97.37±0.064	-	-	3.8	0.05	Training-free
NASI-ADA Shu et al. [2022]	-	97.10±0.13	-	3.7	0.24	Training-free
SWAP Peng et al. [2024]	-	97.52±0.09	-	4.3	0.004	Training-free
APD(C10)	97.63±0.13 ↑(0.13)	-	84.83±0.09 ↑(1.33)	4.4	0.004	Training-free

Method	Top-1(%)	Top-5(%)	Params (M)	FLOPs (M)	GPU-Days	Search method
ResNet50 He et al. [2016]	75.3	92.2	25.6	4100	-	Manual
AmoebaNet-A Zoph et al. [2018]	74.5	92.4	6.4	555	3150	Evolution
ProxylessNAS-RL Cai et al. [2018]	74.6	92.3	5.8	465	8.3	RL
EfficientNet-B0 Tan and Le [2019]	76.3	93.2	5.3	390	≈3000	RL
NASNet-A Zoph et al. [2018]	74.0	91.6	5.3	564	2000	RL
DARTS Liu et al. [2018]	73.3	91.3	4.7	574	4	Gradient
FBNet Wu et al. [2019]	74.9	-	5.5	375	216	Gradient
P-DARTS(C100) Chen et al. [2019]	75.3	92.5	5.1	577	0.3	Gradient
PC-DARTS(Img) Xu et al. [2019]	75.8	92.7	5.3	597	3.7	Gradient
DARTS+ Liang et al. [2019]	76.3	92.8	5.1	591	0.2	Gradient
DARTS-(Img) Chu et al. [2020]	76.2	93.0	4.9	467	4.5	Gradient
FairDARTS-B(Img) Chu et al. [2020]	75.1	92.5	4.8	541	-	Gradient
DARTS+PT(C10) Wang et al. [2021]	74.5	92.0	4.6	-	0.8	Gradient
β-DARTS(C100) Ye et al. [2022]	75.8	92.9	5.4	597	0.4	Gradient
Λ-DARTS Movahedi et al. [2023]	75.7	-	5.2	-	-	Gradient
FP-DARTS(C10) Wang et al. [2023]	75.7	92.7	5.4	-	0.08	Gradient
PDARTS-AER^{ed} Jing et al. [2023]	76.0	92.8	5.1	578	2.0	Gradient
IS-DARTS He et al. [2024]	75.9	92.9	6.4	-	0.42	Gradient
NAO Luo et al. [2018]	74.3	91.8	11.4	584	200	Proxy
TENAS Chen et al. [2021]	75.5	92.5	5.4	-	0.17	Training-free
NASI-ADA(C10) Shu et al. [2022]	75.0	92.2	4.9	559	0.01	Training-free
SWAP Shu et al. [2022] (Img)	76.0	92.4	5.8	-	0.006	Training-free
APD(Img)	76.9 ↑(0.6)	94.0 ↑(0.8)	6.3	695	0.004 ↓(1.5×)	Training-free

4.3 Performance on DARTS Search Space

CIFAR-10 and CIFAR-100 Datasets. As shown in Table 3, APD achieves state-of-the-art performance with significantly reduced search costs. On CIFAR-10, APD attains a top-1 accuracy of 97.63% using merely 0.004 GPU-days, surpassing representative gradient-based methods such as DARTS and advanced training-free methods like TENAS. Similarly, on CIFAR-100, APD achieves 84.83% accuracy, outperforming leading competitors including DARTS+ and FP-DARTS. These results clearly demonstrate that APD sets a new benchmark in both accuracy and search efficiency across datasets.

ImageNet1k Dataset. Table 3 (right) summarizes results on ImageNet1k, demonstrating the strong generalization capability of our method. APD achieves 76.9% top-1 accuracy, improving over the leading training-free method (e.g. NASI-ADA and SWAP) and the existing best one-shot method. Importantly, APD achieves these improvements with a minimal search cost of only 0.004 GPU-days, which is 1.5× less than SWAP. These findings clearly demonstrate APD's excellent performance and generalization efficiency across different datasets.

Table 4: Results on TransNAS-Bench-101-Micro.

Method	Autoencoding	Scene Classification	Jigsaw
	SSIM	Accuracy (%)	Accuracy (%)
Ground Truth	0.58	54.9	95.4
Grad_norm Abdelfattah et al. [2021]	0.36± 0.03	48.7±0.7	80.3±0.3
SNIP Abdelfattah et al. [2021]	0.33±0.04	48.7±1.1	80.3±0.1
Grasp Abdelfattah et al. [2021]	0.33±0.06	50.2±1.6	91.1±0.3
Fisher Abdelfattah et al. [2021]	0.49±0.01	48.7±0.6	83.5±1.2
Synflow Abdelfattah et al. [2021]	0.46±0.07	53.7±1.2	90.9±0.4
NWOT Mellor et al. [2021]	0.43±0.02	53.2±0.6	92.3±0.3
Zen-score Lin et al. [2021]	0.46±0.01	53.7±0.2	87.5±0.4
GradSign Zhang and Jia [2021]	0.35±0.03	53.6±0.4	93.1±0.4
Params	0.46	53.7	85.9
FLOPs	0.46	53.7	85.9
ZiCo Li et al. [2023]	0.48±0.02	53.7±0.4	93.2±0.4
SWAP Peng et al. [2024]	0.42±0.02	45.0±10.9	89.8±5.6
APD	0.54±0.01 ↑(0.06)	54.0±0.6 ↑(0.3)	91.2±0.1 ↓(2)

Table 5: Performance comparison on NAS-Bench-201 (NB-201) search space with CIFAR-10/100, and ImageNet16-120 datasets, and NAS-Bench-101 (NB-101) search space with CIFAR-10 dataset. We report Kendall's τ (KT) and Spearman's ρ (SPR) computed with all candidate architectures. In addition, we report the average independent runs results obtained from our method. The red, blue, and orange indicate the best, second-best, and third-best results, respectively.

Method	CIFAR-10(NB-201)			CIFAR-100(NB-201)			ImageNet16-120(NB-201)			CIFAR10(NB-101)		Runtime (ms/arch)
	SPR	KT	Test acc.(%)	SPR	KT	Test acc.(%)	SPR	KT	Test acc.(%)	SPR	Test acc.(%)	
Params	0.751	0.576	93.61 ± 0.08	0.726	0.552	70.95 ± 0.37	0.690	0.519	41.67 ± 0.64	0.38	92.18 ± 1.53	-
FLOPs	0.733	0.541	93.61 ± 0.08	0.708	0.517	70.95 ± 0.37	0.691	0.517	41.67 ± 0.64	0.67	92.18 ± 1.53	-
Snip Abdelfattah et al. [2021]	0.614	0.455	86.63 ± 3.89	0.618	0.461	56.53 ± 7.56	0.545	0.409	15.13 ± 10.86	0.71	85.41 ± 1.38	45.78
Grasp Abdelfattah et al. [2021]	0.460	0.318	88.01 ± 3.14	0.470	0.329	61.43 ± 7.04	0.406	0.282	30.85 ± 5.66	0.45	87.08 ± 1.40	93.70
Synflow Abdelfattah et al. [2021]	0.769	0.571	93.67 ± 0.39	0.758	0.562	71.70 ± 0.94	0.745	0.553	43.39 ± 3.21	0.38	89.93 ± 2.97	78.26
NWOT Mellor et al. [2021]	0.743	0.557	91.95 ± 1.29	0.769	0.579	68.88 ± 1.60	0.760	0.573	42.31 ± 3.43	0.32	93.16 ± 0.36	36.54
ZenNAS Lin et al. [2021]	0.365	0.283	89.55 ± 1.12	0.338	0.245	64.69 ± 3.86	0.372	0.260	37.18 ± 3.17	0.65	93.06 ± 0.73	30.07
ZiCo Li et al. [2023]	0.784	0.589	93.69 ± 0.07	0.813	0.620	70.63 ± 1.08	0.804	0.614	41.42 ± 0.97	0.65	92.64 ± 0.99	75.50
AZ-NAS Lee and Ham [2024]	0.913	0.741	93.49 ± 0.30	0.900	0.723	70.33 ± 1.16	0.886	0.710	44.34 ± 1.26	0.42	92.01 ± 0.85	69.43
SWAP Peng et al. [2024]	0.810	0.634	90.48 ± 0.94	0.820	0.649	67.13 ± 1.83	0.774	0.610	35.40 ± 3.96	0.44	90.51 ± 2.08	47.61
APD	0.832	0.635	93.76 ± 0.09 ↑(0.07)	0.843	0.654	72.22 ± 0.65 ↑(0.52)	0.817	0.633	45.03 ± 0.76 ↑(0.69)	0.73	93.49 ± 0.34 ↑(0.33)	16.81 ↓(13.26)
Optimal	-	-	94.33 ± 0.08	-	-	73.30 ± 0.20	-	-	46.97 ± 0.19	-	93.87 ± 0.08	-

4.4 Results on TransNAS-Bench-101–Micro

As summarized in Table 4, our method consistently achieves state-of-the-art performance across all three tasks on TransNAS-Bench-101-Micro, highlighting its strong generalization capability heterogeneous downstream tasks. In particular, for the Autoencoding task, our approach attains an SSIM score of 0.54, surpassing leading methods such as ZiCo (0.48), NWOT (0.43), and SWAP (0.42). Similar performance improvements are observed in the Scene Classification and Jigsaw tasks, demonstrating APD's robustness and effectiveness across diverse downstream tasks.

4.5 Generalizability on OoD-ViT-NAS-Ti

To further evaluate the generalizability of our method on vision transformers under Out-of-Distribution (OoD) conditions, we conduct experiments on the OoD-ViT-NAS-Ti search space Ho et al. [2025] across five datasets: ImageNet1k, ImageNet-A, ImageNet-R, ImageNet-D/Texture, and ImageNet-D/Material. All results are averaged over 5 independent runs. As shown in Table 6, APD consistently outperforms prior methods across all OoD settings. Specifically, APD achieves +0.04 higher ρ than NWOT on ImageNet1k, and +0.01 over DSS on ImageNet-D/Texture. On ImageNet-R, APD surpasses all methods with a highest ρ of 0.88, outperforming AutoProx by +0.10 and DSS by +0.07. These results highlight the strong generalizability of APD under distribution shifts, and further confirm the effectiveness of leveraging LLMs to design accurate and robust zero-cost proxies for transformer-based NAS.

Table 6: Correlation on OoD-ViT-NAS-Ti search space.

Method	ImageNet1k	ImageNet-A	ImageNet-R	ImageNet-D/Texture	ImageNet-D/Material
SNIP	0.38	0.51	0.55	-0.06	0.11
Grasp	-0.03	-0.06	-0.07	-0.01	0.03
MeCo	0.48	0.40	0.33	0.09	0.08
CroZe	0.40	0.54	0.60	0.01	0.12
DSS	0.62	0.82	0.81	0.02	0.17
AutoProx	0.67	0.82	0.78	0.05	0.15
NWOT	0.75	0.76	0.74	0.11	0.12
APD	0.79↑(0.04)	0.82	0.88	0.12↑(0.01)	0.15

4.6 Ablation studies

The impact of various LLMs: To scrutinize the impact of various LLMs (i.e., GPT4o, Llama 4), we perform an ablation study of LLMs on the NAS-Bench-201 search space in the CIFAR-10 dataset (As shown Table 7 and the left panel of Fig. 5) and the TransNAS-Bench-101 Micro search space (as shown Fig. 5 right). Specifically, we conduct experiments by averaging 4 independent runs to keep a fair comparison. From Table 7 and Fig. 5, we draw two conclusions: (1) Our APD demonstrates strong robustness across different LLMs. Specifically, APD achieves highly consistent results under different

Table 7: Comparison of APD with different LLMs on NAS-Bench-201 search space in CIFAR-10 dataset.

Method	LLMs	Run 1	Run 2	Run 3	Run 4	Average (ρ)
Naive	GPT4o	60.37	59.74	60.52	61.40	60.51
APD	Claude 3.7	80.90	80.91	82.72	81.91	81.14
APD	Deepseek V3	79.77	80.78	79.77	79.77	80.24
APD	Gemini flash	75.47	73.31	73.50	74.66	75.22
APD	Llama 4	73.04	72.70	72.32	72.95	72.87
APD	GPT4o	81.59	80.96	81.75	82.62	81.10
APD	Grok 3	72.23	79.77	80.78	84.51	79.32

LLMs, showing minimal performance fluctuations across models. Moreover, APD is stable to noise caused by different training settings, further enhancing its reliability in real-world deployment. (2) Compared to Naive method, our APD significantly improves the performance in terms of accuracy. For example, the accuracy of APD with Claude 3.7 is 21.26% higher than the Naive method. The performance improvement can be attributed to our proposed actor–critic reinforcement learning framework, which provides key reasoning and feedback for proxy generation.

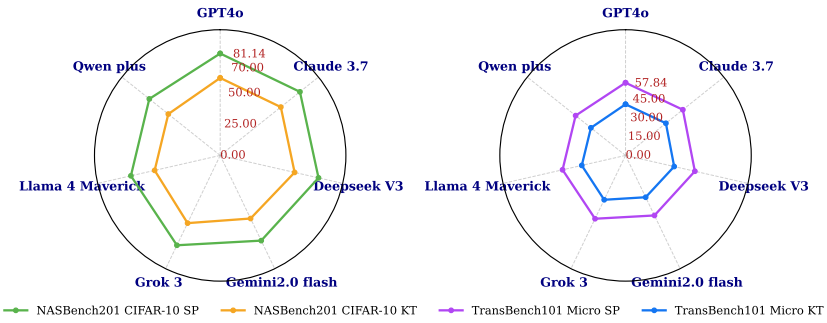

Figure 5: A comparison of ranking correlations of our method designed by 7 mainstream LLMs including GPT4o, Claude 3.7, Deepseek V3, Gemini2.0 flash, Grok 3, Llama 4 Maverick, and Qwen plus. Specifically, we conduct the empirical validation on NAS-Bench-201 (Left) and TransNAS-Bench-101 (Right) search spaces in the CIFAR-10 dataset.

The impact of various components: We conduct ablation studies on NAS-Bench-201 (CIFAR-10/100) to evaluate the effectiveness of key components in APD. As shown in Table 8, the naive version without Evolution and Actor-Critic modules performs poorly (82.04% in CIFAR-10 and 47.62% in CIFAR-100). Introducing Evolution alone significantly boosts performance, yielding +6.49% and +13.54% improvements, respectively. In addition, we observe that there is a joint contribution between Actor-Critic and Evolution. Specifically, ③ obtains 93.76% in CIFAR-10 and 72.22% in CIFAR-100. Those results validate the effectiveness of our APD.

Table 8: Ablation study of various components.

	Naive	Evolution	Actor-Critic	CIFAR-10(NB-201)	CIFAR-100(NB-201)
①	✓	✗	✗	82.04	47.62
②	✓	✓	✗	88.53	61.16
③	✓	✓	✓	93.76	72.22

4.7 Discussion

We are surprised by the remarkable performance of zero-cost proxies designed by LLMs for training-free NAS, in this section, we conduct an in-depth analysis of APD. APD achieves impressive performance primarily due to the effectiveness of the reinforcement learning strategy. The RL policy enables adaptive selection and refinement of zero-cost proxies, guiding the LLM toward generating more task-relevant strategies. This interaction mechanism significantly enhances the synergy between LLMs and NAS, ensuring that the discovered proxies are both generalizable and high-performing.

Despite involving LLMs, our framework mitigates the typical "black-box" concerns by embedding the LLM within an RL-guided optimization loop. This interaction provides a structured feedback signal, reducing the opaqueness of the overall process and making the optimization more transparent and controllable. Moreover, our approach redefines the traditional NAS design paradigm by shifting from handcrafted heuristics to LLM-guided discovery. This not only introduces a new learning framework for NAS but also offers a transferable methodology for other deep learning domains.

4.8 Additional Evaluation

Due to the page limit, we provide more experimental results in **App. A-H**. **❶ Detailed Prompt Engineering of APD** are presented in **App. C**. **❷ More ablation studies** are presented in **App. D**. **❸ Limitations** are presented in **App. E**. **❹ Visualizations of designed AZPs** are presented in **App. F**. **❺ Visualizations of searched architectures** are presented in **App. G**.

Related Work. The related work is provided in **App. H**.

5 Conclusion and Future Works

In this work, we observe that existing zero-cost proxies in training-free NAS are manually crafted, inefficient, and poorly correlated with final performance. To address this, we propose APD, an LLM-driven framework that automatically discovers high-quality proxies without human effort. By incorporating an actor-critic reinforcement learning strategy, APD iteratively refines prompts to generate better proxies. The proposed method achieves state-of-the-art performance and efficiency on multiple NAS benchmarks. We believe APD offers a novel design paradigm and will inspire broader applications of LLMs in automated machine learning. In the future, we plan to further improve the performance of APD.

References

[1] Mohamed S. Abdelfattah, Abhinav Mehrotra, Lukasz Dudziak, and Nicholas Donald Lane. Zero-cost proxies for lightweight NAS. In 9th International Conference on Learning Representations, ICLR 2021, Virtual Event, Austria, May 3-7, 2021. OpenReview.net, 2021.

[2] Josh Achiam, Steven Adler, Sandhini Agarwal, Lama Ahmad, Ilge Akkaya, Florencia Leoni Aleman, Diogo Almeida, Janko Altenschmidt, Sam Altman, Shyamal Anadkat, et al. Gpt-4 technical report. arXiv preprint arXiv:2303.08774, 2023.

[3] Yash Akhauri, J. Pablo Munoz, Nilesh Jain, and Ravi Iyer. Eznas: Evolving zero cost proxies for neural architecture scoring. arXiv preprint arXiv:2209.07413, 2022. URL `https://arxiv.org/abs/2209.07413`.

[4] Anthropic. Claude 3.7 Sonnet. `https://www.anthropic.com/news/claude-3-7-sonnet`, 2025.

[5] Haoyue Bai, Fengwei Zhou, Lanqing Hong, Nanyang Ye, S-H Gary Chan, and Zhenguo Li. Nas-ood: Neural architecture search for out-of-distribution generalization. In Proceedings of the IEEE/CVF International Conference on Computer Vision, pages 8320–8329, 2021.

[6] Tom Brown, Benjamin Mann, Nick Ryder, Melanie Subbiah, Jared D Kaplan, Prafulla Dhariwal, Arvind Neelakantan, Pranav Shyam, Girish Sastry, Amanda Askell, et al. Language models are few-shot learners. Advances in Neural Information Processing Systems, 33:1877–1901, 2020.

[7] Han Cai, Ligeng Zhu, and Song Han. Proxylessnas: Direct neural architecture search on target task and hardware. ArXiv, abs/1812.00332, 2018.

[8] Yupeng Chang, Xu Wang, Jindong Wang, Yuan Wu, Linyi Yang, Kaijie Zhu, Hao Chen, Xiaoyuan Yi, Cunxiang Wang, Yidong Wang, et al. A survey on evaluation of large language models. ACM Transactions on Intelligent Systems and Technology, 15(3):1–45, 2024.

[9] Angelica Chen, David Dohan, and David So. Evoprompting: Language models for code-level neural architecture search. In Advances in Neural Information Processing Systems, volume 36, pages 7787–7817. 2023.

[10] Boyu Chen, Peixia Li, Chuming Li, Baopu Li, Lei Bai, Chen Lin, Ming Sun, Wanli Ouyang, et al. Glit: Neural architecture search for global and local image transformer. In ICCV, 2021.

[11] Minghao Chen, Houwen Peng, Jianlong Fu, and Haibin Ling. Autoformer: Searching transformers for visual recognition. In International Conference on Computer Vision, 2021.

[12] Wuyang Chen, Xinyu Gong, and Zhangyang Wang. Neural architecture search on imagenet in four gpu hours: A theoretically inspired perspective. ArXiv, abs/2102.11535, 2021.

[13] Wuyang Chen, Wei Huang, Xianzhi Du, Xiaodan Song, Zhangyang Wang, and Denny Zhou. Auto-scaling vision transformers without training. In International Conference on Learning Representations, 2022.

[14] Xin Chen, Lingxi Xie, Jun Wu, and Qi Tian. Progressive differentiable architecture search: Bridging the depth gap between search and evaluation. In Proceedings of the IEEE/CVF International Conference on Computer Vision, pages 1294–1303, 2019.

[15] Xiangxiang Chu, Xiaoxing Wang, Bo Zhang, Shun Lu, Xiaolin Wei, and Junchi Yan. Darts-: robustly stepping out of performance collapse without indicators. ArXiv, abs/2009.01027, 2020.

[16] Xiangxiang Chu, Tianbao Zhou, Bo Zhang, and Jixiang Li. Fair darts: Eliminating unfair advantages in differentiable architecture search. In Computer Vision–ECCV 2020: 16th European Conference, Glasgow, UK, August 23–28, 2020, Proceedings, Part XV, pages 465–480. Springer, 2020.

[17] Xiangxiang Chu, Zhi Tian, Bo Zhang, Xinlong Wang, Xiaolin Wei, Huaxia Xia, and Chunhua Shen. Conditional positional encodings for vision transformers. Arxiv preprint 2102.10882, 2021. URL `https://arxiv.org/pdf/2102.10882.pdf`.

[18] Xuanyi Dong and Yi Yang. Nas-bench-201: Extending the scope of reproducible neural architecture search. In 8th International Conference on Learning Representations, ICLR 2020, Addis Ababa, Ethiopia, April 26-30, 2020, 2020.

[19] Alexey Dosovitskiy, Lucas Beyer, Alexander Kolesnikov, Dirk Weissenborn, Xiaohua Zhai, Thomas Unterthiner, Mostafa Dehghani, Matthias Minderer, Georg Heigold, Sylvain Gelly, et al. An image is worth 16x16 words: Transformers for image recognition at scale. In International Conference on Learning Representations, 2020.

[20] Yawen Duan, Xin Chen, Hang Xu, Zewei Chen, Xiaodan Liang, Tong Zhang, and Zhenguo Li. Transnas-bench-101: Improving transferability and generalizability of cross-task neural architecture search. In Proceedings of the IEEE/CVF Conference on Computer Vision and Pattern Recognition, pages 5251–5260, 2021.

[21] Google Cloud. Gemini 2.0 Flash. `https://cloud.google.com/vertex-ai/generative-ai/docs/models/gemini/2-0-flash`, 2025.

[22] Daya Guo, Dejian Yang, Haowei Zhang, Junxiao Song, Ruoyu Zhang, Runxin Xu, Qihao Zhu, Shirong Ma, Peiyi Wang, Xiao Bi, et al. Deepseek-r1: Incentivizing reasoning capability in llms via reinforcement learning. arXiv preprint arXiv:2501.12948, 2025.

[23] Kang Haidong, Ma Lianbo, Chen Pengjun, Yu Guo, Wang Xingwei, and Huang Min. Beyond the limits: Overcoming negative correlation of activation-based training-free nas. In International Conference on Computer Vision, 2025.

[24] Kai Han, An Xiao, Enhua Wu, Jianyuan Guo, Chunjing Xu, and Yunhe Wang. Transformer in transformer. In NeurIPS, 2021.

[25] Hongyi He, Longjun Liu, Haonan Zhang, and Nanning Zheng. Is-darts: Stabilizing darts through precise measurement on candidate importance. In Proceedings of the AAAI Conference on Artificial Intelligence, volume 38, pages 12367–12375, 2024.

[26] Kaiming He, Xiangyu Zhang, Shaoqing Ren, and Jian Sun. Deep residual learning for image recognition. In Proceedings of the IEEE Conference on Computer Vision and Pattern Recognition, pages 770–778, 2016.

[27] Tong He, Zhi Zhang, Hang Zhang, Zhongyue Zhang, Junyuan Xie, and Mu Li. Bag of tricks for image classification with convolutional neural networks. In CVPR, 2019.

[28] Byeongho Heo, Sangdoo Yun, Dongyoon Han, Sanghyuk Chun, Junsuk Choe, and Seong Joon Oh. Rethinking spatial dimensions of vision transformers. In ICCV, 2021.

[29] Sy-Tuyen Ho, Tuan Van Vo, Somayeh Ebrahimkhani, and Ngai-Man Cheung. Vision transformer neural architecture search for out-of-distribution generalization: Benchmark and insights. arXiv preprint arXiv:2501.03782, 2025.

[30] Kun Jing, Luoyu Chen, and Jungang Xu. An architecture entropy regularizer for differentiable neural architecture search. Neural Networks, 158:111–120, 2023.

[31] Haidong Kang. Revisiting neural networks for few-shot learning: A zero-cost nas perspective. In Forty-second International Conference on Machine Learning.

[32] Haidong Kang, Lianbo Ma, Guo Yu, and Shangce Gao. Where and how to enhance: Discovering bit-width contribution for mixed precision quantization. In Proceedings of the Thirty-Fourth International Joint Conference on Artificial Intelligence, 2025.

[33] Junghyup Lee and Bumsub Ham. Az-nas: Assembling zero-cost proxies for network architecture search. In Proceedings of the IEEE/CVF Conference on Computer Vision and Pattern Recognition, pages 5893–5903, 2024.

[34] Namhoon Lee, Thalaiyasingam Ajanthan, and Philip Torr. Snip: Single-shot network pruning based on connection sensitivity. In International Conference on Learning Representations.

[35] Guihong Li, Yuedong Yang, Kartikeya Bhardwaj, and Radu Marculescu. Zico: Zero-shot nas via inverse coefficient of variation on gradients. arXiv preprint arXiv:2301.11300, 2023.

[36] Hanwen Liang, Shifeng Zhang, Jiacheng Sun, Xingqiu He, Weiran Huang, Kechen Zhuang, and Zhenguo Li. Darts+: Improved differentiable architecture search with early stopping. ArXiv, abs/1909.06035, 2019.

[37] Ming Lin, Pichao Wang, Zhenhong Sun, Hesen Chen, Xiuyu Sun, Qi Qian, Hao Li, and Rong Jin. Zen-nas: A zero-shot NAS for high-performance image recognition. In 2021 IEEE/CVF International Conference on Computer Vision, ICCV 2021, Montreal, QC, Canada, October 10-17, 2021, pages 337–346. IEEE, 2021. doi: 10.1109/ICCV48922.2021.00040.

[38] Aixin Liu, Bei Feng, Bing Xue, Bingxuan Wang, Bochao Wu, Chengda Lu, Chenggang Zhao, Chengqi Deng, Chenyu Zhang, Chong Ruan, et al. Deepseek-v3 technical report. arXiv preprint arXiv:2412.19437, 2024.

[39] Chenxi Liu, Barret Zoph, Maxim Neumann, Jonathon Shlens, Wei Hua, Li-Jia Li, Li Fei-Fei, Alan Yuille, Jonathan Huang, and Kevin Murphy. Progressive neural architecture search. In Proceedings of the European Conference on Computer Vision (ECCV), pages 19–34, 2018.

[40] Hanxiao Liu, Karen Simonyan, and Yiming Yang. Darts: Differentiable architecture search. ArXiv, abs/1806.09055, 2018.

[41] Ze Liu, Yutong Lin, Yue Cao, Han Hu, Yixuan Wei, Zheng Zhang, Stephen Lin, and Baining Guo. Swin transformer: Hierarchical vision transformer using shifted windows. In ICCV, 2021.

[42] Renqian Luo, Fei Tian, Tao Qin, Enhong Chen, and Tie-Yan Liu. Neural architecture optimization. Advances in Neural Information Processing Systems, 31, 2018.

[43] L. Ma, H. Kang, G. Yu, Q. Li, and Q. He. Single-domain generalized predictor for neural architecture search system. IEEE Transactions on Computers, 73(05):1400–1413, 2024. ISSN 1557-9956.

[44] Joe Mellor, Jack Turner, Amos Storkey, and Elliot J Crowley. Neural architecture search without training. In International Conference on Machine Learning, pages 7588–7598. PMLR, 2021.

[45] Meta AI. The llama 4 herd: The beginning of a new era of natively multimodal ai innovation. `https://ai.meta.com/blog/llama-4-multimodal-intelligence/`, 2025. Accessed: May 16, 2025.

[46] Sajad Movahedi, Melika Adabinejad, Ayyoob Imani, Arezou Keshavarz, Mostafa Dehghani, Azadeh Shakery, and Babak Nadjar Araabi. λ-darts: Mitigating performance collapse by harmonizing operation selection among cells. In The Eleventh International Conference on Learning Representations, ICLR 2023, Kigali, Rwanda, May 1-5, 2023, 2023.

[47] Muhammad Usama Nasir, Samuel Earle, Julian Togelius, Steven James, and Clayton Cleghorn. Llmatic: Neural architecture search via large language models and quality diversity optimization. In Proceedings of the Genetic and Evolutionary Computation Conference, pages 1110–1118, July 2024.

[48] Yameng Peng, Andy Song, Haytham M Fayek, Vic Ciesielski, and Xiaojun Chang. Swap-nas: Sample-wise activation patterns for ultra-fast nas. arXiv preprint arXiv:2403.04161, 2024.

[49] Yameng Peng, Andy Song, Haytham M. Fayek, Vic Ciesielski, and Xiaojun Chang. SWAP-NAS: Sample-wise activation patterns for ultra-fast NAS. In The Twelfth International Conference on Learning Representations, 2024.

[50] Hieu Pham, Melody Guan, Barret Zoph, Quoc Le, and Jeff Dean. Efficient neural architecture search via parameters sharing. In International Conference on Machine Learning, pages 4095–4104. PMLR, 2018.

[51] Qwen Team. Qwen2.5 technical report. arXiv preprint arXiv:2412.15115, 2024. URL `https://arxiv.org/abs/2412.15115`. Includes the Qwen-Plus Mixture-of-Experts variant.

[52] Alec Radford, Karthik Narasimhan, Tim Salimans, Ilya Sutskever, et al. Improving language understanding by generative pre-training. 2018.

[53] Esteban Real, Alok Aggarwal, Yanping Huang, and Quoc V. Le. Regularized evolution for image classifier architecture search. In AAAI Conference on Artificial Intelligence, volume 33, page 4780–4789, 2019.

[54] Mark Sandler, Andrew Howard, Menglong Zhu, Andrey Zhmoginov, and Liang-Chieh Chen. Mobilenetv2: Inverted residuals and linear bottlenecks. In Proceedings of the IEEE Conference on Computer Vision and Pattern Recognition, pages 4510–4520, 2018.

[55] Yao Shu, Shaofeng Cai, Zhongxiang Dai, Beng Chin Ooi, and Bryan Kian Hsiang Low. NASI: Label- and data-agnostic neural architecture search at initialization. In International Conference on Learning Representations, 2022.

[56] Xiu Su, Shan You, Jiyang Xie, Mingkai Zheng, Fei Wang, Chen Qian, Changshui Zhang, Xiaogang Wang, and Chang Xu. Vision transformer architecture search. In Computer Vision – ECCV 2022: 17th European Conference, Tel Aviv, Israel, October 23–27, 2022, Proceedings, Part XXI, page 139–157, 2022.

[57] Haosen Sun, Lujun Li, Peijie Dong, Zimian Wei, and Shitong Shao. Auto-das: Automated proxy discovery for training-free distillation-aware architecture search. In Computer Vision – ECCV 2024, Lecture Notes in Computer Science, pages 56–73. Springer Cham, 2024. doi: 10.1007/978-3-031-72652-1_4.

[58] Mingxing Tan and Quoc Le. Efficientnet: Rethinking model scaling for convolutional neural networks. In International Conference on Machine Learning, pages 6105–6114. PMLR, 2019.

[59] Hugo Touvron, Matthieu Cord, Matthijs Douze, Francisco Massa, Alexandre Sablayrolles, and Hervé Jégou. Training data-efficient image transformers & distillation through attention. In ICML. PMLR, 2021.

[60] Chaoqi Wang, Guodong Zhang, and Roger Grosse. Picking winning tickets before training by preserving gradient flow. arXiv preprint arXiv:2002.07376, 2020.

[61] Ruochen Wang, Minhao Cheng, Xiangning Chen, Xiaocheng Tang, and Cho-Jui Hsieh. Rethinking architecture selection in differentiable nas. ArXiv, abs/2108.04392, 2021.

[62] Wenhai Wang, Enze Xie, Xiang Li, Deng-Ping Fan, Kaitao Song, Ding Liang, Tong Lu, Ping Luo, and Ling Shao. Pyramid vision transformer: A versatile backbone for dense prediction without convolutions. In ICCV, 2021.

[63] Wenna Wang, Xiuwei Zhang, Hengfei Cui, Hanlin Yin, and Yannnig Zhang. Fp-darts: Fast parallel differentiable neural architecture search for image classification. Pattern Recognition, 136:109193, 2023.

[64] Zimian Wei, Peijie Dong, Zheng Hui, Anggeng Li, Lujun Li, Menglong Lu, Hengyue Pan, and Dongsheng Li. Auto-prox: Training-free vision transformer architecture search via automatic proxy discovery. In Proceedings of the AAAI Conference on Artificial Intelligence, volume 38, pages 15814–15822, 2024.

[65] Bichen Wu, Xiaoliang Dai, Peizhao Zhang, Yanghan Wang, Fei Sun, Yiming Wu, Yuandong Tian, Peter Vajda, Yangqing Jia, and Kurt Keutzer. Fbnet: Hardware-aware efficient convnet design via differentiable neural architecture search. In Proceedings of the IEEE/CVF Conference on Computer Vision and Pattern Recognition, pages 10734–10742, 2019.

[66] xAI. Grok 3: The age of reasoning agents. `https://x.ai/news/grok-3`, 2025.

[67] Guorui Xie, Qing Li, Zhenning Shi, Hanbin Fang, Shengpeng Ji, Yong Jiang, Zhenhui Yuan, Lianbo Ma, and Mingwei Xu. Generating neural networks for diverse networking classification tasks via hardware-aware neural architecture search. IEEE Transactions on Computers, 2023.

[68] Yuhui Xu, Lingxi Xie, Xiaopeng Zhang, Xin Chen, Guo-Jun Qi, Qi Tian, and Hongkai Xiong. Pc-darts: Partial channel connections for memory-efficient architecture search. ArXiv, abs/1907.05737, 2019.

[69] Zhaohui Yang, Yunhe Wang, Xinghao Chen, Boxin Shi, Chao Xu, Chunjing Xu, Qi Tian, and Chang Xu. CARS: continuous evolution for efficient neural architecture search. In 2020 IEEE/CVF Conference on Computer Vision and Pattern Recognition, CVPR 2020, Seattle, WA, USA, June 13-19, 2020, pages 1826–1835. IEEE, 2020.

[70] Peng Ye, Baopu Li, Yikang Li, Tao Chen, Jiayuan Fan, and Wanli Ouyang. $\backslash beta$-darts: Beta-decay regularization for differentiable architecture search. In 2022 IEEE/CVF Conference on Computer Vision and Pattern Recognition (CVPR), pages 10864–10873. IEEE, 2022.

[71] Chris Ying, Aaron Klein, Eric Christiansen, Esteban Real, Kevin Murphy, and Frank Hutter. Nas-bench-101: Towards reproducible neural architecture search. In International Conference on Machine Learning, pages 7105–7114. PMLR, 2019.

[72] Li Yuan, Yunpeng Chen, Tao Wang, Weihao Yu, Yujun Shi, Zihang Jiang, Francis EH Tay, Jiashi Feng, and Shuicheng Yan. Tokens-to-token vit: Training vision transformers from scratch on imagenet. In ICCV, 2021.

[73] Zhihao Zhang and Zhihao Jia. Gradsign: Model performance inference with theoretical insights. arXiv preprint arXiv:2110.08616, 2021.

[74] Xiawu Zheng, Rongrong Ji, Yuhang Chen, Qiang Wang, Baochang Zhang, Jie Chen, Qixiang Ye, Feiyue Huang, and Yonghong Tian. Migo-nas: Towards fast and generalizable neural architecture search. IEEE Transactions on Pattern Analysis and Machine Intelligence, 43(9): 2936–2952, 2021.

[75] Dongzhan Zhou, Xinchi Zhou, Wenwei Zhang, Chen Change Loy, Shuai Yi, Xuesen Zhang, and Wanli Ouyang. Econas: Finding proxies for economical neural architecture search. In 2020 IEEE/CVF Conference on Computer Vision and Pattern Recognition, CVPR 2020, Seattle, WA, USA, June 13-19, 2020, pages 11393–11401. IEEE, 2020.

[76] Qinqin Zhou, Kekai Sheng, Xiawu Zheng, Ke Li, Xing Sun, Yonghong Tian, Jie Chen, and Rongrong Ji. Training-free transformer architecture search. In Proceedings of the IEEE/CVF Conference on Computer Vision and Pattern Recognition, pages 10894–10903, 2022.

[77] Barret Zoph and Quoc V. Le. Neural architecture search with reinforcement learning. In International Conference on Learning Representations (ICLR), 2017.

[78] Barret Zoph, Vijay Vasudevan, Jonathon Shlens, and Quoc V Le. Learning transferable architectures for scalable image recognition. In Proceedings of the IEEE Conference on Computer Vision and Pattern Recognition, pages 8697–8710, 2018.

NeurIPS Paper Checklist

1. **Claims**

   Question: Do the main claims made in the abstract and introduction accurately reflect the paper's contributions and scope?

   Answer: [Yes]

   Justification: The abstract and introduction clearly and accurately reflect the paper's contributions and scope.

   Guidelines:

   - The answer NA means that the abstract and introduction do not include the claims made in the paper.
   - The abstract and/or introduction should clearly state the claims made, including the contributions made in the paper and important assumptions and limitations. A No or NA answer to this question will not be perceived well by the reviewers.
   - The claims made should match theoretical and experimental results, and reflect how much the results can be expected to generalize to other settings.
   - It is fine to include aspirational goals as motivation as long as it is clear that these goals are not attained by the paper.

2. **Limitations**

   Question: Does the paper discuss the limitations of the work performed by the authors?

   Answer: [Yes]

   Justification: Our limitations are in section 5.

   Guidelines:

   - The answer NA means that the paper has no limitation while the answer No means that the paper has limitations, but those are not discussed in the paper.
   - The authors are encouraged to create a separate "Limitations" section in their paper.
   - The paper should point out any strong assumptions and how robust the results are to violations of these assumptions (e.g., independence assumptions, noiseless settings, model well-specification, asymptotic approximations only holding locally). The authors should reflect on how these assumptions might be violated in practice and what the implications would be.
   - The authors should reflect on the scope of the claims made, e.g., if the approach was only tested on a few datasets or with a few runs. In general, empirical results often depend on implicit assumptions, which should be articulated.
   - The authors should reflect on the factors that influence the performance of the approach. For example, a facial recognition algorithm may perform poorly when image resolution is low or images are taken in low lighting. Or a speech-to-text system might not be used reliably to provide closed captions for online lectures because it fails to handle technical jargon.
   - The authors should discuss the computational efficiency of the proposed algorithms and how they scale with dataset size.
   - If applicable, the authors should discuss possible limitations of their approach to address problems of privacy and fairness.
   - While the authors might fear that complete honesty about limitations might be used by reviewers as grounds for rejection, a worse outcome might be that reviewers discover limitations that aren't acknowledged in the paper. The authors should use their best judgment and recognize that individual actions in favor of transparency play an important role in developing norms that preserve the integrity of the community. Reviewers will be specifically instructed to not penalize honesty concerning limitations.

3. **Theory assumptions and proofs**

   Question: For each theoretical result, does the paper provide the full set of assumptions and a complete (and correct) proof?

   Answer: [Yes]

Justification: The full set of assumptions and complete proofs are provided in section 3.

Guidelines:

- The answer NA means that the paper does not include theoretical results.
- All the theorems, formulas, and proofs in the paper should be numbered and cross-referenced.
- All assumptions should be clearly stated or referenced in the statement of any theorems.
- The proofs can either appear in the main paper or the supplemental material, but if they appear in the supplemental material, the authors are encouraged to provide a short proof sketch to provide intuition.
- Inversely, any informal proof provided in the core of the paper should be complemented by formal proofs provided in appendix or supplemental material.
- Theorems and Lemmas that the proof relies upon should be properly referenced.

4. **Experimental result reproducibility**

   Question: Does the paper fully disclose all the information needed to reproduce the main experimental results of the paper to the extent that it affects the main claims and/or conclusions of the paper (regardless of whether the code and data are provided or not)?

   Answer: [Yes]

   Justification: This paper provide sufficient information to reproduce the main experiments.

   Guidelines:

   - The answer NA means that the paper does not include experiments.
   - If the paper includes experiments, a No answer to this question will not be perceived well by the reviewers: Making the paper reproducible is important, regardless of whether the code and data are provided or not.
   - If the contribution is a dataset and/or model, the authors should describe the steps taken to make their results reproducible or verifiable.
   - Depending on the contribution, reproducibility can be accomplished in various ways. For example, if the contribution is a novel architecture, describing the architecture fully might suffice, or if the contribution is a specific model and empirical evaluation, it may be necessary to either make it possible for others to replicate the model with the same dataset, or provide access to the model. In general. releasing code and data is often one good way to accomplish this, but reproducibility can also be provided via detailed instructions for how to replicate the results, access to a hosted model (e.g., in the case of a large language model), releasing of a model checkpoint, or other means that are appropriate to the research performed.
   - While NeurIPS does not require releasing code, the conference does require all submissions to provide some reasonable avenue for reproducibility, which may depend on the nature of the contribution. For example
     (a) If the contribution is primarily a new algorithm, the paper should make it clear how to reproduce that algorithm.
     (b) If the contribution is primarily a new model architecture, the paper should describe the architecture clearly and fully.
     (c) If the contribution is a new model (e.g., a large language model), then there should either be a way to access this model for reproducing the results or a way to reproduce the model (e.g., with an open-source dataset or instructions for how to construct the dataset).
     (d) We recognize that reproducibility may be tricky in some cases, in which case authors are welcome to describe the particular way they provide for reproducibility. In the case of closed-source models, it may be that access to the model is limited in some way (e.g., to registered users), but it should be possible for other researchers to have some path to reproducing or verifying the results.

5. **Open access to data and code**

   Question: Does the paper provide open access to the data and code, with sufficient instructions to faithfully reproduce the main experimental results, as described in supplemental material?

Answer: [Yes]

Justification: We provided runnable code in the supplementary material.

Guidelines:

- The answer NA means that paper does not include experiments requiring code.
- Please see the NeurIPS code and data submission guidelines (`https://nips.cc/public/guides/CodeSubmissionPolicy`) for more details.
- While we encourage the release of code and data, we understand that this might not be possible, so "No" is an acceptable answer. Papers cannot be rejected simply for not including code, unless this is central to the contribution (e.g., for a new open-source benchmark).
- The instructions should contain the exact command and environment needed to run to reproduce the results. See the NeurIPS code and data submission guidelines (`https://nips.cc/public/guides/CodeSubmissionPolicy`) for more details.
- The authors should provide instructions on data access and preparation, including how to access the raw data, preprocessed data, intermediate data, and generated data, etc.
- The authors should provide scripts to reproduce all experimental results for the new proposed method and baselines. If only a subset of experiments are reproducible, they should state which ones are omitted from the script and why.
- At submission time, to preserve anonymity, the authors should release anonymized versions (if applicable).
- Providing as much information as possible in supplemental material (appended to the paper) is recommended, but including URLs to data and code is permitted.

6. **Experimental setting/details**

   Question: Does the paper specify all the training and test details (e.g., data splits, hyperparameters, how they were chosen, type of optimizer, etc.) necessary to understand the results?

   Answer: [Yes]

   Justification: All experimental details and settings are in Appendix B.

   Guidelines:

   - The answer NA means that the paper does not include experiments.
   - The experimental setting should be presented in the core of the paper to a level of detail that is necessary to appreciate the results and make sense of them.
   - The full details can be provided either with the code, in appendix, or as supplemental material.

7. **Experiment statistical significance**

   Question: Does the paper report error bars suitably and correctly defined or other appropriate information about the statistical significance of the experiments?

   Answer: [Yes]

   Justification: The error bars reported in our paper are appropriately and clearly defined.

   Guidelines:

   - The answer NA means that the paper does not include experiments.
   - The authors should answer "Yes" if the results are accompanied by error bars, confidence intervals, or statistical significance tests, at least for the experiments that support the main claims of the paper.
   - The factors of variability that the error bars are capturing should be clearly stated (for example, train/test split, initialization, random drawing of some parameter, or overall run with given experimental conditions).
   - The method for calculating the error bars should be explained (closed form formula, call to a library function, bootstrap, etc.)
   - The assumptions made should be given (e.g., Normally distributed errors).
   - It should be clear whether the error bar is the standard deviation or the standard error of the mean.

- It is OK to report 1-sigma error bars, but one should state it. The authors should preferably report a 2-sigma error bar than state that they have a 96% CI, if the hypothesis of Normality of errors is not verified.
- For asymmetric distributions, the authors should be careful not to show in tables or figures symmetric error bars that would yield results that are out of range (e.g. negative error rates).
- If error bars are reported in tables or plots, The authors should explain in the text how they were calculated and reference the corresponding figures or tables in the text.

8. **Experiments compute resources**

   Question: For each experiment, does the paper provide sufficient information on the computer resources (type of compute workers, memory, time of execution) needed to reproduce the experiments?

   Answer: [Yes]

   Justification: Sufficient information is included in the paper to reproduce all experimental results.

   Guidelines:

   - The answer NA means that the paper does not include experiments.
   - The paper should indicate the type of compute workers CPU or GPU, internal cluster, or cloud provider, including relevant memory and storage.
   - The paper should provide the amount of compute required for each of the individual experimental runs as well as estimate the total compute.
   - The paper should disclose whether the full research project required more compute than the experiments reported in the paper (e.g., preliminary or failed experiments that didn't make it into the paper).

9. **Code of ethics**

   Question: Does the research conducted in the paper conform, in every respect, with the NeurIPS Code of Ethics `https://neurips.cc/public/EthicsGuidelines`?

   Answer: [Yes]

   Justification: Our research fully adheres to the NeurIPS Code of Ethics.

   Guidelines:

   - The answer NA means that the authors have not reviewed the NeurIPS Code of Ethics.
   - If the authors answer No, they should explain the special circumstances that require a deviation from the Code of Ethics.
   - The authors should make sure to preserve anonymity (e.g., if there is a special consideration due to laws or regulations in their jurisdiction).

10. **Broader impacts**

    Question: Does the paper discuss both potential positive societal impacts and negative societal impacts of the work performed?

    Answer: [NA]

    Justification: There is no societal impact of the work performed.

    Guidelines:

    - The answer NA means that there is no societal impact of the work performed.
    - If the authors answer NA or No, they should explain why their work has no societal impact or why the paper does not address societal impact.
    - Examples of negative societal impacts include potential malicious or unintended uses (e.g., disinformation, generating fake profiles, surveillance), fairness considerations (e.g., deployment of technologies that could make decisions that unfairly impact specific groups), privacy considerations, and security considerations.

- The conference expects that many papers will be foundational research and not tied to particular applications, let alone deployments. However, if there is a direct path to any negative applications, the authors should point it out. For example, it is legitimate to point out that an improvement in the quality of generative models could be used to generate deepfakes for disinformation. On the other hand, it is not needed to point out that a generic algorithm for optimizing neural networks could enable people to train models that generate Deepfakes faster.
- The authors should consider possible harms that could arise when the technology is being used as intended and functioning correctly, harms that could arise when the technology is being used as intended but gives incorrect results, and harms following from (intentional or unintentional) misuse of the technology.
- If there are negative societal impacts, the authors could also discuss possible mitigation strategies (e.g., gated release of models, providing defenses in addition to attacks, mechanisms for monitoring misuse, mechanisms to monitor how a system learns from feedback over time, improving the efficiency and accessibility of ML).

11. **Safeguards**

    Question: Does the paper describe safeguards that have been put in place for responsible release of data or models that have a high risk for misuse (e.g., pretrained language models, image generators, or scraped datasets)?

    Answer: [NA]

    Justification: This paper poses no such risks.

    Guidelines:

    - The answer NA means that the paper poses no such risks.
    - Released models that have a high risk for misuse or dual-use should be released with necessary safeguards to allow for controlled use of the model, for example by requiring that users adhere to usage guidelines or restrictions to access the model or implementing safety filters.
    - Datasets that have been scraped from the Internet could pose safety risks. The authors should describe how they avoided releasing unsafe images.
    - We recognize that providing effective safeguards is challenging, and many papers do not require this, but we encourage authors to take this into account and make a best faith effort.

12. **Licenses for existing assets**

    Question: Are the creators or original owners of assets (e.g., code, data, models), used in the paper, properly credited and are the license and terms of use explicitly mentioned and properly respected?

    Answer: [NA]

    Justification: We mention the license in the README file in the code of the provided supplementary material.

    Guidelines:

    - The answer NA means that the paper does not use existing assets.
    - The authors should cite the original paper that produced the code package or dataset.
    - The authors should state which version of the asset is used and, if possible, include a URL.
    - The name of the license (e.g., CC-BY 4.0) should be included for each asset.
    - For scraped data from a particular source (e.g., website), the copyright and terms of service of that source should be provided.
    - If assets are released, the license, copyright information, and terms of use in the package should be provided. For popular datasets, `paperswithcode.com/datasets` has curated licenses for some datasets. Their licensing guide can help determine the license of a dataset.
    - For existing datasets that are re-packaged, both the original license and the license of the derived asset (if it has changed) should be provided.

- If this information is not available online, the authors are encouraged to reach out to the asset's creators.

13. **New assets**

    Question: Are new assets introduced in the paper well documented and is the documentation provided alongside the assets?

    Answer: [NA]

    Justification: This paper does not release new assets.

    Guidelines:

    - The answer NA means that the paper does not release new assets.
    - Researchers should communicate the details of the dataset/code/model as part of their submissions via structured templates. This includes details about training, license, limitations, etc.
    - The paper should discuss whether and how consent was obtained from people whose asset is used.
    - At submission time, remember to anonymize your assets (if applicable). You can either create an anonymized URL or include an anonymized zip file.

14. **Crowdsourcing and research with human subjects**

    Question: For crowdsourcing experiments and research with human subjects, does the paper include the full text of instructions given to participants and screenshots, if applicable, as well as details about compensation (if any)?

    Answer: [NA]

    Justification: This paper does not involve crowdsourcing nor research with human subjects.

    Guidelines:

    - The answer NA means that the paper does not involve crowdsourcing nor research with human subjects.
    - Including this information in the supplemental material is fine, but if the main contribution of the paper involves human subjects, then as much detail as possible should be included in the main paper.
    - According to the NeurIPS Code of Ethics, workers involved in data collection, curation, or other labor should be paid at least the minimum wage in the country of the data collector.

15. **Institutional review board (IRB) approvals or equivalent for research with human subjects**

    Question: Does the paper describe potential risks incurred by study participants, whether such risks were disclosed to the subjects, and whether Institutional Review Board (IRB) approvals (or an equivalent approval/review based on the requirements of your country or institution) were obtained?

    Answer: [NA]

    Justification: We does not involve crowdsourcing nor research with human subjects.

    Guidelines:

    - The answer NA means that the paper does not involve crowdsourcing nor research with human subjects.
    - Depending on the country in which research is conducted, IRB approval (or equivalent) may be required for any human subjects research. If you obtained IRB approval, you should clearly state this in the paper.
    - We recognize that the procedures for this may vary significantly between institutions and locations, and we expect authors to adhere to the NeurIPS Code of Ethics and the guidelines for their institution.
    - For initial submissions, do not include any information that would break anonymity (if applicable), such as the institution conducting the review.

16. **Declaration of LLM usage**

Question: Does the paper describe the usage of LLMs if it is an important, original, or non-standard component of the core methods in this research? Note that if the LLM is used only for writing, editing, or formatting purposes and does not impact the core methodology, scientific rigorousness, or originality of the research, declaration is not required.

Answer: [Yes]

Justification: We describe our prompt engineering workflow using LLMs as a core component in section 3.

Guidelines:

- The answer NA means that the core method development in this research does not involve LLMs as any important, original, or non-standard components.
- Please refer to our LLM policy (`https://neurips.cc/Conferences/2025/LLM`) for what should or should not be described.

A A Simple Prompt

To empirically validate the hypothesis presented in Section 2, we employ the prompt depicted in Figure 6 to assess the capability of LLMs in generating effective ZCPs.

Figure 6: A representative minimal prompt used in our naive experiments.

Prompt for Naive

Please help me design **five novel Zero-Cost Proxies** for evaluating the **expressive performance** of a neural network on a given batch of image data using **training-free metrics**.

These proxies should require **no training**, and must be computationally cheap to evaluate, similar to existing zero-cost proxy methods such as **NWOT**, **SynFlow**, or **Jacobian Covariance**. However, you should not **copy or imitate** these methods — your goal is to **creatively propose original ideas** that align with the following requirements:

For each of the **five proxies**, do the following:
Firstly, provide a **one-paragraph description** of the idea, including how the score is computed.
Secondly, Implement the proxy in **Python**, as a function named 'evaluate(model, data)' that: Takes a neural network object ('model')(pytorch model) and image batch ('data')(tensor) as input. Returns a scalar score ('score') reflecting expressive performance.

Note: Do **not** use training. Avoid random sampling or stochastic components. The heuristic must work on general-purpose image data and standard neural networks (e.g., CNNs). **Do not** provide any additional explanation outside of the required description and code.

B Experimental settings

B.1 Evolution Settings

Table 9 summarizes the default hyper-parameter configuration used in APD evolutionary experiments. Searches are conducted on a single RTX4090 GPU with a fixed random seed of 0. Each candidate proxy's performance is averaged over 5 independent forward passes using a batch of 16 random samples. We adopt CIFAR-10 as the primary benchmark and report transfer results on CIFAR-10 and ImageNet-16. The actor-critic controller is a two layer MLP with 256 hidden units. The actor and critic learning rates are set to 1e-3 and 1e-2, respectively, with a discount factor $\gamma = 0.9$. During search we run 10 episodes of 100 steps search and test every individual for 200 architectures. The controller retains a history window of 5.

Table 9: Hyper-parameters for Automatic Proxy Discovery.

Parameter	Value	Parameter	Value
Episodes	10	Steps	100
History windows	5	Discount factor	0.9
Actor learning rate	1e-3	Critic learning rate	1e-2
Input batch size	16	Repeats	5
Hidden size	256	Number of layers	2
Population size	5	β	1

B.2 DARTS Settings

We list the training hyper-parameters we adopt for all experiments on DARTS. Figure 27 shows the optimal architecture obtained by APD in the DARTS search space.

As detailed in Table 10, models are trained for 600 epochs with a fixed random seed of 42. We employ SGD with momentum 0.9, an initial learning rate of 0.025 that is decayed to zero via cosine annealing, weight decay of 5e-4, and gradient clipping at a maximum norm of 5. Architectures begin

Table 10: Hyper-parameters for DARTS training.

Parameter	Value	Parameter	Value
Seed	42	Batch size	96
CutOut length	16	Initial channels	36
Cells / layers	20	Aux. loss weight	0.4
Learning rate	0.025	Momentum	0.9
Weight decay	5e-4	Grad clip (norm)	5
DropPath prob.	0.2	Lr scheduler	CosineAnnealing

with 36 channels and stack 20 cells. An auxiliary classifier is attached with a loss weight of 0.4. We apply CutOut regularization (length=16) and linearly increase DropPath probability 0.2 over the course of training. All runs use a batch size of 96.

B.3 Autoformer Settings

For all ImageNet-1k training runs, we adhere to the core setup prescribed by AutoFormer [69], which is listed in Table 11. The subnet discovered by APD are reported in Figure 28, Figure 29 and Figure 30.

We retrain discovered AutoFormer architectures for 300 epochs on ImageNet-1k using AdamW with an initial learning rate of 5e-4, cosine decay to 1e-5, and a 5 epoch warm-up. The network consumes 224×224 images split into 16×16 patches, and optimization runs with a batch of 128. Regularization follows the AutoFormer baseline. RandAugment (9 transformations, magnitude 0.5), mixup-cutmix blending ($\alpha = 0.8$, switch probability 0.5), random erasing (probability 0.25, pixel model), and a linearly ramped drop-path of 0.1. All experiments use the retrain mode, thereby only the chosen subnet's weights are updated while the supernet is frozen.

Table 11: Hyper-parameter configuration used to retrain the subnet on ImageNet-1K.

Category	Parameter	Value	Notes
Data	Input resolution	224×224	—
	Patch size	16	ViT patch size
	Batch size	128	—
Optimiser	Optimizer	AdamW	$\beta = (0.9, 0.999)$, $\epsilon = 10^{-8}$
	Initial LR	5e-4	Scaled by batch size / 512
	Weight decay	0.05	Decoupled
	LR schedule	Cosine	5 warm-up + 300 epochs
Regularisation	Drop-path rate	0.10	Linearly increased
	RandAugment	`rand-m9-mstd0.5-inc1`	Timm default
	Mixup / CutMix	α=0.8, prob. = 1	Switch prob. = 0.5
Model	Training mode	*retrain*	Only subnet weights updated
	Max rel. position	14	Bias radius

B.4 LLMs Settings

For proxy generation, we interface with GPT-4o via the Chat Completion API [2] and evaluate APD across multiple LLMs, including Claude 3.7 [4], Grok 3 [66], Gemini 2.0 Flash [21], Deepseek V3 [38], and Qwen Plus [51]. To balance diversity and syntactic correctness, APD is performed with a temperature of 0.5 and the output length is capped at 8192 tokens. We supply a specialized system prompt that constrains LLM to emit JSON object with two fields: thought + code.

C Prompt Engineering

In this section, we outline the guiding principles underlying the design of our prompts. Given that the effectiveness of LLM-driven heuristic discovery critically hinges on prompt quality, our prompts are carefully crafted to maintain clarity, specificity, and structured output. Particularly, we ensure clarity and specificity by precisely defining the computational boundaries and structural properties of

candidate proxies within each prompt, clearly delineating the allowable search space of the metrics to facilitate efficient exploration by the LLM. Inspired by previous auto proxy discovery research, we prompt the LLM to construct compositional proxies represented as directed acyclic graphs that integrate network-derived signals (e.g., gradients, activations, or weights) with basic statistical and arithmetic operations. Collectively, this rigorous prompt engineering strategy significantly enhances the efficiency, validity, and innovativeness of the ZCPs by APD.

Moreover, through extensive empirical experimentation, we observe that the initial code representation of a generated ZCP typically fails to fully realize its underlying conceptual potential. Specifically, the initial instantiation of the proxy, directly produces from a single prompt, often exhibits suboptimal correlation with the final performance metrics. It is only after applying evolutionary strategies such as mutation and crossover operations that iteratively refine the proxy structure and composition that the intrinsic effectiveness of the proxy becomes evident. This empirical insight underscores the necessity of iterative exploration and refinement within the APD, highlighting mutation and crossover as critical mechanisms for achieving robust and effective ZCPs.

C.1 Prompt For NAS-Bench-201

We provide the detailed prompts employed in our experiments on NAS-Bench-201 [18]. These prompts serve as explicit instructions guiding the LLM to systematically generate novel ZCPs. Specifically, we design three variants of prompts as depicted in Figure 7, 8, and 9. Each prompt variant progressively introduces structured definitions, constraints on computational operations, and explicit guidelines to ensure that the generated proxies adhere to our framework requirements, thereby facilitating effective exploration of the proxy search space and enhancing the quality of the discovered ZCPs.

C.2 Prompt For TransNAS-Bench-101

We detail the specific prompts utilized for proxy discovery experiments on TransNAS-Bench-101 [20]. These prompts are carefully crafted to instruct the large language model (LLM) to produce novel zero-cost proxies tailored specifically for their diverse tasks, including JIGSAW, autoencoding, scene classification, and object classification. To accommodate these distinct downstream tasks, we designed three prompt variants as shown in Figure 10, 11 and 12.

C.3 Prompt For AutoFormer

We present the detailed prompts employed for proxy discovery experiments conducted on the AutoFormer architecture search space. Given AutoFormer's specific structural characteristics and its transformer-based design for vision tasks, we carefully tailor three distinct prompt variants following previous designs in Figure 13, 14 and 15.

D Extended Experimental Results

D.1 Additional Ablation Studies

Analysis on Mutation and Crossover operations To figure out the roles of the mutation and crossover operations, we evaluate the individual contribution of the mutation and crossover operation by selectively disabling each component during proxy search and observing the resulting performance changes. Figure 12 illustrates that omitting the mutation prompt reduces the proxy's correlation with ground-truth metrics while removal of the crossover operation narrows the architectural exploration space and weakens proxy accuracy. These findings confirm that mutation and crossover provide distinct but complementary functions. collectively enabling the effective of high-quality zero-cost proxies.

Analysis on population size To understand how the size of the evolving population affects the quality and convergence of our zero-cost proxy search, we perform an ablation study over three different population sizes: 1, 2, 3, 4, 5 and 10. A larger population can offer richer diversity and robustness but incurs greater computational overhead and makes it harder for the LLM to follow context, thereby reducing ZCPs quality.In contrast, a smaller population accelerates each generation

Figure 7: Prompt used for intialization in NAS-Bench-201.

Prompt for Initialization

Your Task: Please design **5 Zero-Cost Proxies** to evaluate the representation capability of different convolutional network architectures on a given dataset. The final goal of each proxy is to provide a **scalar score** that reflects the performance of a given network. You should generate Zero-Cost Proxies according to the following specifications, which include: **proxy requirements**, **description of the proxy search space** (defining the structure of how the proxy is computed), **the search space of the networks being evaluated**, the **given dataset**, and the **output format**, as described below:

Proxy Requirements:
Training-free: No gradient descent, weight updates, or learned parameters
Efficient: Low computational cost, suitable for early-stage model selection
Dxeterministic: No stochastic elements or randomness
Input-aware: The proxy should utilize a batch of input image data
Model-sensitive: The proxy should reflect meaningful differences between models.

Proxy Search Space: The computation of the proxy can be represented as a **directed acyclic graph (DAG)**. For any given node, its in-degree must satisfy $0 \leq degree_{in} \leq 2$.
Nodes with only outgoing edges and no incoming edges are called **inputs**. Inputs consist of two parts: the input module and the input property. The input module refers to different types of network layers (e.g., convolutional layers, BatchNorm, activation layers, etc.), and the input property is one of the following: gradient G, weights W, or output feature maps Z. An input is defined as a combination of these two components. For example, (convolutional layer + gradient G) refers to the gradients of the convolutional layer's parameters. A proxy can have multiple inputs.
Nodes with both incoming and outgoing edges are referred to as **operations**, which are further divided into two types:

- When $degree_{in} = 1$, the node typically performs a **statistical operation** such as computing the mean or standard deviation of the preceding node's output.
- When $degree_{in} = 2$, the node typically performs a **binary operation**, such as addition, subtraction, or division between two inputs.
- Nodes with only incoming edges are **outputs**. There must be **only one output node** in the DAG. The input to this final node must be a **scalar**.

Network Search Space: Networks drawn from NASBench-201, varying only in cell structure. Macro architecture: input → conv → cell_n → residual (stride=2) → cell_n → residual (stride=2) → cell_∗n → global average pooling. Cells: DAGs of four nodes with operations: zeroize, skip-connection, 1×1 conv, 3×3 conv, 3×3 avg-pool.

Given Dataset: CIFAR-10 classification with input shape (3×32×32) and 10-dimensional output.

Output: For each proxy, provide a **Description** paragraph and **Code** demo implementing `evaluate(model, inputs, targets)` in PyTorch. Ensure numerical stability, deterministic outputs, and move any returned tensors to CPU.

Note: Your Zero-Cost Proxies must not be the same as any existing ones (such as nwot, snip, etc.), though you may draw inspiration from them. Ensure numerical stability in your functions (avoid inf or nan during computation). Do not provide any additional explanation outside of the required description and code.

but risks premature convergence. We fix all other settings and report the average Spearman correlation between proxy scores in Table 13.

Analysis on hyperparameter To assess how the discount factor γ and the history window size affect proxy quality, we conduct two separate ablations, one varying γ over $\{0.5, 0.7, 0.9, 0.99\}$, and the other varying the history window over $\{1, 3, 5, 10\}$. All other settings remain fixed. Results are reported in Table 14 and Table 15.

Analysis on actor-critic To evaluate the effect of varying the number of hidden layers in the actor-critic controller on proxy search performance and convergence speed, we conduct an ablation over depths of 2, 3, 4, and 5 layers. Table 16 reports the final Spearman correlation achieved after

Figure 8: Prompt used for mutation in NAS-Bench-201.

Prompt for Mutation

Your Task: Building upon the initial set of **Zero-Cost Proxies**, you will now perform a **mutation** step to generate novel and distinct proxies. You should introduce creative variations into existing proxies through systematic modifications. Follow the mutation rules and constraints defined below to design **5 distinct mutated proxies**:

Mutation Rules: When mutating a proxy, you must choose at least **one** and up to **four** of the following mutations to apply:

- **Input Mutation**: Replace, add, or remove one type of input (e.g., switch from convolutional layer gradients (G) to activation outputs (Z)). Consider using less commonly utilized inputs such as BatchNorm statistics or residual block outputs.
- **Operation Mutation**: Change statistical operations (mean, variance, max, min) to another statistic. Substitute binary operations (+, -, , /) with different arithmetic operations, ensuring numerical stability.
- **Structure Mutation**: Adjust the computational graph by altering the connections (edges) between nodes, ensuring the DAG property remains valid. Introduce an additional intermediate node for richer representations.
- **Aggregation Mutation**: Modify how multiple layer values are aggregated (e.g., sum, mean, weighted average).

Mutated Proxy Search Space:

- Each node has an in-degree $0 \leq degree_{in} \leq 2$.
- Exactly **one output node** producing a scalar value.
- Inputs: Combinations of modules (conv, BatchNorm, activation layers, residual block outputs) and properties (gradients G, weights W, outputs Z).
- Operations: Statistical (mean, variance, max, min, sum) or binary (+, -, , /).

Network Search Space: Networks drawn from NASBench-201, varying only in cell structure. Macro architecture: input $\rightarrow$ conv $\rightarrow$ cell_n $\rightarrow$ residual (stride=2) $\rightarrow$ cell_n $\rightarrow$ residual (stride=2) $\rightarrow$ cell_$*$n $\rightarrow$ global average pooling. Cells: DAGs of four nodes with operations: zeroize, skip-connection, 1×1 conv, 3×3 conv, 3×3 avg-pool.

Given Dataset: CIFAR-10 classification with input shape (3×32×32) and 10-dimensional output.

Output: For each proxy, provide a **Description** paragraph and **Code** demo implementing `evaluate(model, inputs, targets)` in PyTorch. Ensure numerical stability, deterministic outputs, and move any returned tensors to CPU.

Note: Do **not** use training. Avoid random sampling or stochastic components. The heuristic must work on general-purpose image data and standard neural networks (e.g., CNNs). **Do not** provide any additional explanation outside of the required description and code.

Existing Proxies:
<Existing Proxies>

convergence and the generation at which the search stabilized for each depth. The results indicate that evolution planning itself is relatively straightforward. A two-layer actor-critic controller already achieves convergence within 50 generations. Employing additional layers results in an increased number of ineffective generations, incurring unnecessary computational overhead without further improving performance (e.g., in the later stages of evolution when proxy quality improvements become minimal, continuing with fixed initialization procedures can result in diminishing returns, incurring unnecessary computational overhead).

Figure 9: Prompt used for crossover in NAS-Bench-201.

Prompt for Crossover

Your Task: Expanding upon the previously defined Zero-Cost Proxies, your next step is to implement a **crossover** operation to create novel proxies. The crossover process involves combining aspects of **two parent proxies** to produce **5 distinct crossover proxies**. Adhere to the crossover rules and constraints defined below:

Crossover Rules: To generate crossover proxies, select two parent proxies from previously defined proxies. Apply at least **one** and up to **two** of the following crossover techniques:

- **Input Crossover**: Exchange input nodes between parent proxies, such as combining gradients (G) from one proxy and outputs (Z) from another.
- **Operation Crossover**: Merge operation nodes by replacing a statistical or binary operation from one parent with an operation from the other parent.
- **Structure Crossover**: Blend the computational graph structures of two proxies by interchanging node connections, ensuring the resulting DAG remains valid.
- **Aggregation Crossover**: Combine aggregation strategies (e.g., sum, mean, weighted average) from the two parent proxies.

Crossover Proxy Search Space:

- Nodes must have an in-degree $0 \leq degree\_in \leq 2$.
- Exactly **one output node** producing a scalar value.
- Inputs: combinations of modules (conv, BatchNorm, activation layers, residual block outputs) and properties (gradients G, weights W, outputs Z).
- Operations: statistical (mean, variance, max, min, sum) or binary (+, -, , /).

Network Search Space: Networks drawn from NASBench-201, varying only in cell structure. Macro architecture: input $\rightarrow$ conv $\rightarrow$ cell_n $\rightarrow$ residual (stride=2) $\rightarrow$ cell_n $\rightarrow$ residual (stride=2) $\rightarrow$ cell_$*$n $\rightarrow$ global average pooling. Cells: DAGs of four nodes with operations: zeroize, skip-connection, 1×1 conv, 3×3 conv, 3×3 avg-pool.

Output: For each proxy, provide a **Description** paragraph and **Code** demo implementing `evaluate(model, inputs, targets)` in PyTorch. Ensure numerical stability, deterministic outputs, and move any returned tensors to CPU.

Note: Do **not** use training. Avoid random sampling or stochastic components. The heuristic must work on general-purpose image data and standard neural networks (e.g., CNNs). **Do not** provide any additional explanation outside of the required description and code.

Existing Proxies:
<Existing Proxies>

D.2 Detailed Cross-LLM Performance

We track the evolution of average Spearman correlation over 20 generations for each LLM backbone under. Table 17 reports the per-generation correlation on NAS-Bench-201 for all seven models.

D.3 AutoFormer Accuracy Results

We evaluate the architectures discovered by APD in the AutoFormer search space on ImageNet–1k classification. Table 18 reports the Top-1 accuracies for the tiny, small, and base variants: the tiny model achieves 76.1 %, the small model 81.5 %. These results demonstrate that our search not only produces proxies with high correlation to ground truth but also yields architectures that deliver competitive performance on a large-scale vision benchmark.

Figure 10: Prompt for initialization in TransNAS-Bench-101.

Prompt for Initialization

Your Task: Please design **5 novel Zero-Cost proxies** to evaluate the representation capability of different convolutional network architectures on a given downstream task. The final goal of each proxy is to provide a **scalar score** that reflects the performance of a given network. You should generate Zero-Cost Proixes according to the following specifications, which include: **proxy requirements**, **description of the proxy search space** (defining the structure of how the proxy is computed), the **search space of the networks being evaluated**, the **given dataset**, and the **output format**, as described below:

Proxy Requirements:

- **Training-free**: No gradient descent, weight updates, or learned parameters.
- **Efficient**: Low computational cost, suitable for early-stage model selection.
- **Deterministic**: No stochastic elements or randomness.
- **Model-sensitive**: The proxy should reflect meaningful differences between models.

Proxy Search Space: The computation of the proxy can be represented as a **directed acyclic graph (DAG**. For any given node, its in-degree must satisfy $0 \leq degree_{in} \leq 2$.
Nodes with only outgoing edges and no incoming edges are called **inputs**. Inputs consist of two parts: the input module and the input property. The input module refers to different types of network layers (e.g., convolutional layers, BatchNorm, activation layers, etc.), and the input property is one of the following: gradient G, weights W, or output feature maps Z. An input is defined as a combination of these two components. For example, (convolutional layer + gradient G) refers to the gradients of the convolutional layer's parameters. A proxy can have multiple inputs.
Nodes with both incoming and outgoing edges are referred to as **operations**, which are further divided into two types:

- When $degree_{in} = 1$, the node typically performs a **statistical operation** such as computing the mean or standard deviation of the preceding node's output.
- When $degree_{in} = 2$, the node typically performs a **binary operation**, such as addition, subtraction, or division between two inputs.

Nodes with only incoming edges are **outputs**. There must be **only one output node** in the DAG. The input to this final node must be a **scalar**.

Network Search Space: The networks to be evaluated come from **TransNAS-Bench-101**, which includes variations in both **cell-level** and **macro-level structures**.
Macro architecture: img $\rightarrow$ searched backbone (composed of stacked cells) $\rightarrow$ task-specific decoder. The macro structure consists of **three stages**, each containing **modules** made of **residual blocks**. After each stage, downsampling and channel doubling occur. For example: Stage 1 (Module 1) $\rightarrow$ residual blocks $\rightarrow$ Stage 2 (Module 2, 3) $\rightarrow$ residual blocks $\rightarrow$ Stage 3 (Module 4) $\rightarrow$ residual blocks $\rightarrow$ task-specific head.
Cell structure: Each cell is modeled as a **directed acyclic graph (DAG)** with six nodes. For any $v_i, v_j \in V$, if $i < j$, then $e_{ij} \in E$. Each node represents a latent feature tensor, and each edge represents a candidate operation from the following set:

- zeroize
- skip-connection
- 1 × 1 convolution
- 3 × 3 convolution

Each cell forms the base unit of the backbone and is repeatedly stacked according to the macro-level configuration. This enables flexible network designs across different tasks such as object classification, semantic segmentation, surface normal estimation, and more.

Given Downstream Task:
<Given Downstream Task>

Figure 11: Prompt for mutation in TransNAS-Bench-101.

Prompt for Mutation

Your Task: Building upon the initial set of **Zero-Cost Proxies**, you will now perform a **mutation** step to generate novel and distinct proxies. You should introduce creative variations into existing proxies through systematic modifications. Follow the mutation rules and constraints defined below to design **5 distinct mutated proxies**:
Mutation Rules: When mutating a proxy, you must choose at least **one** and up to **four** of the following mutations to apply:

- **Input Mutation**: Replace, add, or remove one type of input (e.g., switch from convolutional layer gradients (G) to activation outputs (Z)). Consider using less commonly utilized inputs such as BatchNorm statistics or residual block outputs.
- **Operation Mutation**: Change statistical operations (mean, variance, max, min) to another statistic. Substitute binary operations (+, -, , /) with different arithmetic operations, ensuring numerical stability.
- **Structure Mutation**: Adjust the computational graph by altering the connections (edges) between nodes, ensuring the DAG property remains valid.Introduce an additional intermediate node for richer representations.
- **Aggregation Mutation**: Modify how multiple layer values are aggregated (e.g., sum, mean, weighted average).

Proxy Search Space: The computation of the proxy can be represented as a **directed acyclic graph (DAG**. For any given node, its in-degree must satisfy $0 \leq degree_{in} \leq 2$.
Nodes with only outgoing edges and no incoming edges are called **inputs**. Inputs consist of two parts: the input module and the input property. The input module refers to different types of network layers (e.g., convolutional layers, BatchNorm, activation layers, etc.), and the input property is one of the following: gradient G, weights W, or output feature maps Z. An input is defined as a combination of these two components. For example, (convolutional layer + gradient G) refers to the gradients of the convolutional layer's parameters. A proxy can have multiple inputs.
Nodes with both incoming and outgoing edges are referred to as **operations**, which are further divided into two types:

- When $degree_{in} = 1$, the node typically performs a **statistical operation** such as computing the mean or standard deviation of the preceding node's output.
- When $degree_{in} = 2$, the node typically performs a **binary operation**, such as addition, subtraction, or division between two inputs.

Nodes with only incoming edges are **outputs**. There must be **only one output node** in the DAG. The input to this final node must be a **scalar**.

Network Search Space: The networks to be evaluated come from **TransNAS-Bench-101**, which includes variations in both **cell-level** and **macro-level structures**.
Macro architecture: img $\rightarrow$ searched backbone (composed of stacked cells) $\rightarrow$ task-specific decoder. The macro structure consists of **three stages**, each containing **modules** made of **residual blocks**. After each stage, downsampling and channel doubling occur. For example: Stage 1 (Module 1) $\rightarrow$ residual blocks $\rightarrow$ Stage 2 (Module 2, 3) $\rightarrow$ residual blocks $\rightarrow$ Stage 3 (Module 4) $\rightarrow$ residual blocks $\rightarrow$ task-specific head.
Cell structure: Each cell is modeled as a **directed acyclic graph (DAG)** with six nodes. For any $v_i, v_j \in V$, if $i < j$, then $e_{ij} \in E$. Each node represents a latent feature tensor, and each edge represents a candidate operation from the following set:

- zeroize
- skip-connection
- 1 × 1 convolution
- 3 × 3 convolution

Each cell forms the base unit of the backbone and is repeatedly stacked according to the macro-level configuration. This enables flexible network designs across different tasks such as object classification, semantic segmentation, surface normal estimation, and more.

Given Downstream Task:
<Given Downstream Task>

Figure 12: Prompt for crossover in TransNAS-Bench-101.

Prompt for Crossover

Your Task: Expanding upon the previously defined Zero-Cost Proxies, your next step is to implement a **crossover** operation to create novel proxies. The crossover process involves combining aspects of **two parent proxies** to produce **5 distinct crossover proxies**. Adhere to the crossover rules and constraints defined below:

Crossover Rules: To generate crossover proxies, select two parent proxies from previously defined or mutated proxies. Apply at least **one** and up to **two** of the following crossover techniques:

- **Input Crossover**: Exchange input nodes between parent proxies, such as combining gradients (G) from one proxy and outputs (Z) from another.
- **Operation Crossover**: Blend the computational graph structures of two proxies by interchanging node connections, ensuring the resulting DAG remains valid.
- **Structure Crossover**: Blend the computational graph structures of two proxies by interchanging node connections, ensuring the resulting DAG remains valid.
- **Aggregation Crossover**: Combine aggregation strategies (e.g., sum, proxies.

Proxy Search Space: The computation of the proxy can be represented as a **directed acyclic graph (DAG**. For any given node, its in-degree must satisfy $0 \leq degree_{in} \leq 2$.
Nodes with only outgoing edges and no incoming edges are called **inputs**. Inputs consist of two parts: the input module and the input property. The input module refers to different types of network layers (e.g., convolutional layers, BatchNorm, activation layers, etc.), and the input property is one of the following: gradient G, weights W, or output feature maps Z. An input is defined as a combination of these two components. For example, (convolutional layer + gradient G) refers to the gradients of the convolutional layer's parameters. A proxy can have multiple inputs.
Nodes with both incoming and outgoing edges are referred to as **operations**, which are further divided into two types:

- When $degree_{in} = 1$, the node typically performs a **statistical operation** such as computing the mean or standard deviation of the preceding node's output.
- When $degree_{in} = 2$, the node typically performs a **binary operation**, such as addition, subtraction, or division between two inputs.

Nodes with only incoming edges are **outputs**. There must be **only one output node** in the DAG. The input to this final node must be a **scalar**.

Network Search Space: The networks to be evaluated come from **TransNAS-Bench-101**, which includes variations in both **cell-level** and **macro-level structures**.
Macro architecture: img $\rightarrow$ searched backbone (composed of stacked cells) $\rightarrow$ task-specific decoder. The macro structure consists of **three stages**, each containing **modules** made of **residual blocks**. After each stage, downsampling and channel doubling occur. For example: Stage 1 (Module 1) $\rightarrow$ residual blocks $\rightarrow$ Stage 2 (Module 2, 3) $\rightarrow$ residual blocks $\rightarrow$ Stage 3 (Module 4) $\rightarrow$ residual blocks $\rightarrow$ task-specific head.
Cell structure: Each cell is modeled as a **directed acyclic graph (DAG)** with six nodes. For any $v_i, v_j \in V$, if $i < j$, then $e_{ij} \in E$. Each node represents a latent feature tensor, and each edge represents a candidate operation from the following set:

- zeroize
- skip-connection
- 1 × 1 convolution
- 3 × 3 convolution

Each cell forms the base unit of the backbone and is repeatedly stacked according to the macro-level configuration. This enables flexible network designs across different tasks such as object classification, semantic segmentation, surface normal estimation, and more.

Given Downstream Task:
<Given Downstream Task>

Figure 13: Prompt for initialization in AutoFormer.

Prompt for Initialization

Your Task: Please design **5 novel Zero-Cost Proxies** to evaluate the representation capability of different transformer network architectures on a given dataset. The final goal of each proxy is to provide a **scalar score** that reflects the performance of a given network. You should generate zero-cost proxies according to the following specifications, which include: **proxy requirements**, **description of the proxy search space** (defining the structure of how the metric is computed), the **search space of the networks being evaluated**, the **given dataset**, and the **output format**, as described below:

Proxy Requirements:

- **Training-free**: No gradient descent, weight updates, or learned parameters.
- **Efficient**: Low computational cost, suitable for early-stage model selection.
- **Deterministic**: No stochastic elements or randomness.
- **Model-sensitive**: The proxy should reflect meaningful differences between models.

Proxy Search Space: The computation of the proxy can be represented as a **directed acyclic graph (DAG)**. For any given node, its in-degree must satisfy $0 \leq degree_{in} \leq 2$.
Nodes with only outgoing edges and no incoming edges are called **inputs**. Inputs consist of two parts: the input module and the input property. The input module refers to different types of network layers, and the input property is one of the following: gradient G, weights W, or output feature maps Z. An input is defined as a combination of these two components. For example, (convolutional layer + gradient G) refers to the gradients of the convolutional layer's parameters. A proxy can have multiple inputs.
Nodes with both incoming and outgoing edges are referred to as **operations**, which are further divided into two types:

- When $degree_{in} = 1$, the node typically performs a **statistical operation** such as computing the mean or standard deviation of the preceding node's output.
- When $degree_{in} = 2$, the node typically performs a **binary operation**, such as addition, subtraction, or division between two inputs.

Nodes with only incoming edges are **outputs**. There must be **only one output node** in the DAG. The input to this final node must be a **scalar**.

Search Space: The search space defines a set of possible architectural configurations derived from the supernet. Instead of fixed parameters, it provides discrete choices or ranges for each architectural hyperparameter, enabling the selection or evaluation of optimal subnetworks.
A typical search space includes the following parameters with explicit candidate values:

- **EMBED DIM**: A set of embedding dimensions ($D \in \{D_1, D_2, \ldots, D_n\}$), e.g., ($D \in \{528, 576, 624\}$).
- **NUM HEADS**: Choices for attention heads ($H \in \{H_1, H_2, \ldots, H_m\}$), e.g., ($H \in \{9, 10\}$).
- **MLP RATIO**: Options for the MLP expansion ratio ($R_{mlp} \in \{R_1, R_2, \ldots, R_k\}$), e.g., ($R_{mlp} \in \{3.0, 3.5, 4.0\}$).
- **DEPTH**: Number of transformer blocks ($L \in \{L_1, L_2, \ldots, L_s\}$), e.g., ($L \in \{14, 15, 16\}$).

Formally, the search space $\mathcal{A}$ can be defined as a Cartesian product of discrete hyperparameter sets: $\mathcal{A} = \{(D, H, R_{mlp}, L) \mid D \in \{528, 576, 624\}, H \in \{9, 10\}, R_{mlp} \in \{3.0, 3.5, 4.0\}, L \in \{14, 15, 16\}\}$

Given Dataset: The architectures will be evaluated on an image classification task using **IMAGE-NET**. The input image shape is **(3, 224, 224)**, and the network outputs a **1000-dimensional vector**.

Note: Your Zero-Cost Proxies must not be the same as any existing ones (such as nwot, snip, etc.), though you may draw inspiration from them. Ensure numerical stability in your functions (avoid inf or nan during computation).

Figure 14: Prompt for mutation in AutoFormer.

Prompt for Mutation

Your Task: Given **5 existing Zero-Cost proxies**, **mutate** each of these proxies to create **5 new ones** (one mutated version per original proxy). Each mutated proxy should still be **training-free**, **computationally efficient**, **deterministic**, **input-aware**, and **model-sensitive**. The final goal is to produce **5 updated or extended training-free proxies** that remain valid for early-stage model selection but differ in approach from the original set.
When generating each mutated proxy, you may:

- Slightly alter or combine existing nodes in the computation DAG
- Introduce new operations or input types (still abiding by the in-degree constraints)
- Change the nature of the final scalar computation
- Ensure numerical stability (avoid division by zero, log of non-positive numbers, etc.)

Proxy Requirements:

- **Training-free**: Do **not** use any form of parameter updates.
- **Efficient**: Maintain low overhead in computation.
- **Deterministic**: Must produce consistent outputs for the same model and data.
- **Model-sensitive**: Should vary meaningfully with different subnetworks sampled from the supernet.

Proxy Search Space: All mutated proxies should still form a **directed acyclic graph (DAG)** in their computation. For any given node:

- **In-degree Constraint**: $0 \leq degree_{in} \leq 2$.
- **Input Nodes**: Consist of a network module. Tied to a property (W, G, or Z). You may now choose to introduce new input properties that are still relevant to a training-free scenario (e.g., a logarithm of weights, or a combined dimension of feature maps), but be sure to keep them deterministic and valid.
- **Operation Nodes (single-operand)**: Perform statistical transformations (e.g., mean, variance, norms, etc.).
- **Operation Nodes (binary)**: Perform pairwise operations (e.g., addition, multiplication, ratio).
- **Output Node**: Must be a single scalar value (with no outgoing edges).

Search Space: The search space defines a set of possible architectural configurations derived from the supernet. Instead of fixed parameters, it provides discrete choices or ranges for each architectural hyperparameter, enabling the selection or evaluation of optimal subnetworks.
A typical search space includes the following parameters with explicit candidate values:

- **EMBED DIM**: A set of embedding dimensions ($D \in \{D_1, D_2, \ldots, D_n\}$), e.g., ($D \in \{528, 576, 624\}$).
- **NUM HEADS**: Choices for attention heads ($H \in \{H_1, H_2, \ldots, H_m\}$), e.g., ($H \in \{9, 10\}$).
- **MLP RATIO**: Options for the MLP expansion ratio ($R_{mlp} \in \{R_1, R_2, \ldots, R_k\}$), e.g., ($R_{mlp} \in \{3.0, 3.5, 4.0\}$).
- **DEPTH**: Number of transformer blocks ($L \in \{L_1, L_2, \ldots, L_s\}$), e.g., ($L \in \{14, 15, 16\}$).

Formally, the search space $\mathcal{A}$ can be defined as a Cartesian product of discrete hyperparameter sets: $\mathcal{A} = \{(D, H, R_{mlp}, L) \mid D \in \{528, 576, 624\}, H \in \{9, 10\}, R_{mlp} \in \{3.0, 3.5, 4.0\}, L \in \{14, 15, 16\}\}$

Given Dataset: The architectures will be evaluated on an image classification task using **IMAGE-NET**. The input image shape is **(3, 224, 224)**, and the network outputs a **1000-dimensional vector**.

Note: Your Zero-Cost Proxies must not be the same as any existing ones (such as nwot, snip, etc.), though you may draw inspiration from them. Ensure numerical stability in your functions (avoid inf or nan during computation).

Existing Proxies:
<Existing Proxies>

Figure 15: Prompt for crossover in AutoFormer.

Prompt for Crossover

Your Task: Please design **5 novel Zero-Cost Proxies** to evaluate the representation capability of different transformer network architectures on a given dataset, **using a crossover-based approach**. This means each of your new proxies should be created by **combining at least two distinct ideas, components, or sub-nodes** from hypothetical or existing parent proxies. For instance, if you have two parent proxies A and B with specific inputs or operations, you must form a new child proxy by **merging** relevant parts from each parent, ensuring the final proxy remains logically consistent and provides a **scalar score** that reflects the performance of a given network. You should generate Zero-Cost Proxies according to the following specifications, which include: **proxy requirements**, **description of the proxy search space**, the **search space of the networks being evaluated**, the **given dataset**, and the **output format**, as described below:

Proxy Requirements:

- **Training-free**: Do **not** use any form of parameter updates.
- **Efficient**: Maintain low overhead in computation.
- **Deterministic**: Must produce consistent outputs for the same model and data.
- **Model-sensitive**: Should vary meaningfully with different subnetworks sampled from the supernet.
- **Crossover-based**: Each proxy must **inherit or merge** conceptual "genes" (e.g., particular input sources or operations) from **at least two parent proxies**, forming a new, valid proxy design.

Proxy Search Space: All mutated proxies should still form a **directed acyclic graph (DAG)** in their computation. For any given node:

- **In-degree Constraint**: $0 \leq degree_{in} \leq 2$.
- **Input Nodes**: Consist of a network module. Tied to a property (W, G, or Z). You may now choose to introduce new input properties that are still relevant to a training-free scenario (e.g., a logarithm of weights, or a combined dimension of feature maps), but be sure to keep them deterministic and valid.
- **Operation Nodes (single-operand)**: Perform statistical transformations (e.g., mean, variance, norms, etc.).
- **Operation Nodes (binary)**: Perform pairwise operations (e.g., addition, multiplication, ratio).
- **Output Node**: Must be a single scalar value (with no outgoing edges).

Search Space: The search space defines a set of possible architectural configurations derived from the supernet. Instead of fixed parameters, it provides discrete choices or ranges for each architectural hyperparameter, enabling the selection or evaluation of optimal subnetworks.
A typical search space includes the following parameters with explicit candidate values:

- **EMBED DIM**: A set of embedding dimensions ($D \in \{D_1, D_2, \ldots, D_n\}$), e.g., ($D \in \{528, 576, 624\}$).
- **NUM HEADS**: Choices for attention heads ($H \in \{H_1, H_2, \ldots, H_m\}$), e.g., ($H \in \{9, 10\}$).
- **MLP RATIO**: Options for the MLP expansion ratio ($R_{mlp} \in \{R_1, R_2, \ldots, R_k\}$), e.g., ($R_{mlp} \in \{3.0, 3.5, 4.0\}$).
- **DEPTH**: Number of transformer blocks ($L \in \{L_1, L_2, \ldots, L_s\}$), e.g., ($L \in \{14, 15, 16\}$).

Formally, the search space $\mathcal{A}$ can be defined as a Cartesian product of discrete hyperparameter sets: $\mathcal{A} = \{(D, H, R_{mlp}, L) \mid D \in \{528, 576, 624\}, H \in \{9, 10\}, R_{mlp} \in \{3.0, 3.5, 4.0\}, L \in \{14, 15, 16\}\}$

Given Dataset: The architectures will be evaluated on an image classification task using **IMAGE-NET**. The input image shape is **(3, 224, 224)**, and the network outputs a **1000-dimensional vector**.

Note: Your Zero-Cost Proxies must not be the same as any existing ones (such as nwot, snip, etc.), though you may draw inspiration from them. Ensure numerical stability in your functions (avoid inf or nan during computation).

Table 12: Average proxy correlation over 20 generations for different prompt operations on NAS-Bench-201. Full denotes the complete operation configuration, incorporating both mutation and crossover.

Generation	No Crossover	No Mutation	Full
1	0.444	0.193	**0.246**
2	0.533	0.237	**0.470**
3	0.533	0.349	**0.617**
4	0.533	0.439	**0.628**
5	0.541	0.463	**0.662**
6	0.541	0.463	**0.662**
7	0.541	0.463	**0.705**
8	0.572	0.463	**0.705**
9	0.627	0.547	**0.754**
10	0.640	0.547	**0.794**
11	0.640	0.547	**0.800**
12	0.640	0.669	**0.800**
13	0.640	0.713	**0.800**
14	0.640	0.761	**0.800**
15	0.640	0.761	**0.800**
16	0.680	0.780	**0.800**
17	0.714	0.780	**0.803**
18	0.739	0.780	**0.803**
19	0.739	0.780	**0.813**
20	0.758	0.780	**0.813**

Table 13: Effect of population size on the average Spearman correlation of the full prompt configuration over 20 generations.

Population Size	Avg. Spearman ρ
1	0.6023
2	0.6837
3	0.7541
4	0.8013
5	**0.8124**
10	0.7895

E Limitations

While APD markedly advances training-free NAS, several caveats remain. We group them here for clarity.

Black-box optimization Because APD delegates the generation of every candidate proxy to a LLM, the token-level reasoning that maps a prompt to executable code is not observable, raising black-box concerns. We acknowledge that the LLM itself remains opaque. Nevertheless, APD is designed so that its outer optimization loop is inspectable. The LLM's outputs are evaluated by a public fitness function, and the actor–critic scheduler is trained only on this scalar reward. All decisions that influence the search trajectory therefore pass through a measurable, task-specific signal rather than hidden logits. Thus, while some inner LLM reasoning remains inaccessible, the information APD exposes is already adequate for transparency and troubleshooting, so the residual opacity of LLM is unlikely to undermine the method's value.

Need for a small ground-truth subset Computing fitness requires baseline accuracies for roughly 2-3% of each benchmark, which is standard in NAS studies and inexpensive compared with full training. Although a small ground-truth subset is indispensable for APD, we have empirically shown that the ZCPs obtained on one such subset continue to generalize when transferred to search space with no significant differences. Consequently, even for previously unseen NAS tasks, the overhead introduced by APD remains minimal and well within acceptable bounds.

Prompt-context length growth on very large searches The generator receives at most C_t proxies per step, and both prompt and context are explicitly bounded to fit the LLM window. Empirically the

Table 14: Effect of discount factor γ on average Spearman correlation. Best value is highlighted in yellow.

Discount Factor γ	Avg. Spearman ρ
0.50	0.7124
0.70	0.7823
0.90	**0.8137**
0.99	0.8015

Table 15: Effect of history window size on average Spearman correlation. Best value is highlighted in yellow.

History Window	Avg. Spearman ρ
1	0.6987
3	0.8042
5	**0.8259**
10	0.7791

combined length stayed under 6k tokens in specific population size, and we have to down-sample the context if future domains require longer code.

Security and stability when executing LLM-generated code Each proxy is arbitrary code and could, in principle, issue unsafe or resource-hungry calls. Therefore, code has to be run inside a resource-capped sandbox.

F Discovered AZPs

F.1 Proxy for NAS-Bench-201

To demonstrate the effectiveness of our approach, we present three representative proxies that achieved strong performance on NAS-Bench-201, which are illustrated in Figures 16, 17, and 18.

F.2 Proxy for TransNAS-Bench-101

We present the zero-cost proxies discovered on TransNAS-Bench-101 by APD in Figure 19, 20, and 21.

F.3 Proxy for AutoFormer

In Figure 22, 23, and 24, we present the zero-cost proxies discovered through APD on AutoFormer.

G Searched Architectures

In the DARTS search space, the optimal architecture discovered by APD is shown in Figure 27, with its normal and reduction cells visualized in Figures 25 and 26, respectively. In the AutoFormer setting, the architectures found for the tiny, small, and base variants are presented in Figure 28, 29, and 30, respectively.

H Related Work

H.1 Neural Architecture Search

Neural Architecture Search (NAS) aims to seek high-performance neural networks in an automatic manner. Early works cast the problem as black-box reinforcement learning or evolutionary optimization. NASNet [77] and AmoebaNet [53] trained thousands of architectures from scratch on large GPU clusters, demonstrating the promise of search but at prohibitive cost. Subsequent one-shot methods

Table 16: Impact of A2C network depth on proxy search quality and convergence.

Hidden Layers	Final Spearman ρ	Convergence Generation
2	0.8216	42
3	0.8367	79
4	0.8175	96
5	0.8230	103

Table 17: Evolution of average Spearman correlation over 20 generations on NAS-Bench-201 for different LLM backbones.

Gen.	Claude 3.7	Gemini 2.0 Flash	GPT-4o	Deepseek V3	Qwen Plus	Grok 3	Llama4
1	0.0000	0.3460	0.0989	0.0853	0.0228	0.1293	0.0000
2	0.5040	0.4290	0.1091	0.1720	0.0732	0.1293	0.1319
3	0.5040	0.5027	0.1816	0.1720	0.1292	0.1293	0.1319
4	0.5040	0.5560	0.3909	0.1720	0.3230	0.1293	0.1319
5	0.6553	0.5560	0.4312	0.2126	0.3807	0.1293	0.1319
6	0.7087	0.6033	0.4312	0.2126	0.3807	0.1293	0.1319
7	0.7304	0.6212	0.5036	0.3189	0.3962	0.2669	0.1319
8	0.7304	0.6714	0.6028	0.4923	0.5244	0.2669	0.1319
9	0.7304	0.6714	0.6278	0.4969	0.5518	0.2669	0.1319
10	0.7304	0.6714	0.6806	0.6531	0.6109	0.4071	0.1605
11	0.7713	0.6869	0.7411	0.6531	0.6303	0.6933	0.1605
12	0.7713	0.6869	0.7411	0.6531	0.6303	0.6933	0.1605
13	0.7713	0.6869	0.7744	0.7944	0.6303	0.6933	0.2809
14	0.7713	0.6986	0.7898	0.7944	0.6303	0.7081	0.2809
15	0.7728	0.7317	0.7898	0.7944	0.6439	0.7395	0.3011
16	0.7728	0.7317	0.8090	0.8024	0.6439	0.7395	0.4225
17	0.8114	0.7317	0.8090	0.8024	0.6994	0.7395	0.4348
18	0.8114	0.7517	0.8090	0.8024	0.7212	0.7395	0.5598
19	0.8114	0.7517	0.8090	0.8024	0.7212	0.7697	0.6495
20	0.8114	0.7522	0.8110	0.8024	0.7212	0.7697	0.6973

reduce cost by sharing parameters into a single supernet. ENAS [75] introduces weight sharing with a recurrent controller, while DARTS [40] relaxes the discrete search space to a differentiable mixture, enabling gradient-based updates but inheriting optimization bias and collapse issues that spawned a line of robust variants. However, performance estimation remains the key throughput bottleneck [44].

H.2 Zero-Cost Proxies

NAS traditionally relies on partial or full training to judge candidate models, making large-scale exploration prohibitive. Zero-Cost Proxies (ZCPs) address this bottleneck by estimating an architecture's potential from its randomly initialized weights in significantly less time and constitute a standard component of training-free NAS. The earliest ZCPs exploit gradient saliency. SNIP [34] evaluates weights with the first-order loss sensitivities, GraSP [1] extends the idea to second-order information, and SynFlow [1] removes data dependence by propagating an all-ones input, yielding strong correlations in deep convolutional spaces. A second strand replaces gradients with cheap statistics of activations or parameter layouts. NWOT [44] measures neural-tangent-kernel overlap, Zen-score [37] evaluates Jacobian log-determinants, while ZiCo [35] shows that even simple norms such as parameter count or FLOPs can outperform many hand-crafted heuristics once appropriately normalized.

Despite steady progress, two limitations persist. Firstly, all existing proxies are manually specified. Their functional form rarely transfers intact across tasks (e.g., from NAS-Bench-201 CIFAR10 to TransNAS-Bench-101 autoencoding). Secondly, correlation improvements have largely plateaued, and gains often come at the cost of additional forward passes or Jacobian computations.

H.3 Automatic Proxy Discovery

Automatic Proxy Discovery aims to relieve experts from hand-crafting ZCPs by treating the proxy itself as the search object. The most systematic effort so far is Auto-Prox [64]. It encodes a proxy as a computation graph whose nodes are primitive arithmetic or operations (e.g., exp, log). An evolutionary algorithm with elitism preservation mutates these graphs to maximize a joint correlation

Table 18: The comparison results on the Autoformer search space in the ImageNet dataset. $*$ denotes the results reported by [28].

Models	#Param (M)	FLOPS (B)	Top-1 (%)	Top-5 (%)	Model Type	Design Type	Years	GPU Days
Tiny search space								
ResNet-18* [26]	11.7	1.8	72.5	-	CNNs	Manual	2015	-
MobileNet-V3 [54]	5.5	-	75.2	-	CNNs	Manual	2015	-
Deit-Ti [59]	5.7	1.2	72.2	91.1	Transformer	Manual	2015	-
TNT-Ti [24]	6.1	1.4	73.9	91.9	Transformer	Manual	2015	-
ViT-Ti [19]	5.7	-	74.5	-	Transformer	Manual	ICLR2020	-
CPVT-Ti [17]	6.0	-	74.9	92.6	Transformer	Manual	2015	-
PVT-Tiny [62]	13.2	1.9	75.1	-	Transformer	Manual	2015	-
AutoFormer-Ti [11]	5.7	1.3	74.7	92.6	Transformer	Auto	CVPR2021	24
GLiT-Ti [10]	7.2	1.4	76.3	-	Hybrid	Auto	ICCV2021	N/A
ViTAS-C [56]	5.6	1.3	74.7	91.6	Transformer	Auto	ECCV2022	32
TF-TAS-Ti [76]	5.9	1.4	75.3	92.8	Transformer	Auto	CVPR2022	0.5
Auto-Prox [64]	6.4	-	75.6	-	Transformer	Auto	AAAI2024	0.1
AZ-NAS [33]	6.2	1.4	76.4	-	Transformer	Auto	CVPR2024	0.04
CET-TAS (Ours)	8.4	1.9	76.1	93.1	Transformer	Auto	-	0.25
Small search space								
ResNet-50* [26]	25.6	4.1	80.2	-	CNNs	Manual	2015	-
RegNetY-4GF [27]	20.6	-	79.4	-	CNNs	Manual	2015	-
DeiT-S [59]	22.1	4.7	79.9	95.0	Transformer	Manual	2015	-
ViT-S/16 [19]	22.1	4.7	78.8	-	Transformer	Manual	2015	-
PVT-Small [62]	24.5	3.8	79.8	-	Transformer	Manual	2015	-
Swin-T [41]	29.0	4.5	81.3	-	Transformer	Manual	2015	-
TNT-S [24]	23.8	5.2	81.5	95.7	Transformer	Manual	2015	-
CPVT-S [17]	23.0	-	81.5	95.7	Transformer	Manual	2015	-
T2T-ViT_t-14 [72]	21.5	-	81.7	-	Transformer	Manual	2015	-
AutoFormer-S [11]	22.9	5.1	81.7	95.7	Transformer	Auto	CVPR2021	24
GLiT-S [10]	24.6	4.4	80.5	-	Hybrid	Auto	ICCV2021	N/A
ViTAS-F [56]	27.6	6.0	80.5	95.1	Transformer	Auto	ECCV2022	32
TF-TAS-S [76]	22.8	5.0	81.9	95.8	Transformer	Auto	CVPR2022	0.5
AZ-NAS [33]	23.8	5.1	82.2	-	Transformer	Auto	CVPR2024	0.07
CET-TAS (Ours)	30.9	6.3	81.5	95.3	Transformer	Auto	-	0.25

objective. Auto-Prox, however, is specialized to ViTs. Its search space hard-codes transformer-specific primitives. Similar variants, such as EZNAS [3] and Auto-DAS [57] follow identical graph enumeration but remain tied to fixed settings, respectively, limiting cross-domain portability and placing heavy reliance on human expertise.

H.4 LLM for Neural Architecture Search

Recent research has explored leveraging large language models to assist or even automate the neural architecture search process. EvoPrompting [9] pioneers this direction by treating NAS as a code-level program synthesis task, where LLMs evolve architecture generation programs through an evolutionary prompt-tuning mechanism. By iteratively mutating and refining code snippets that specify architectural design choices, EvoPrompting enables LLMs to autonomously discover performant neural architectures without explicit gradient-based optimization. Building on this paradigm, LLMatic [47] combines LLM-driven architecture generation with quality-diversity optimization, allowing the search process to balance exploration and exploitation more effectively. Through LLM-guided mutation and recombination, LLMatic produces diverse yet high-performing architectures across vision and reinforcement learning benchmarks. Collectively, these works demonstrate that LLMs hold substantial potential for application in neural architecture search, suggesting that language-driven reasoning can serve as a viable mechanism for exploring the search space.

However, a critical limitation of these approaches lies in their reliance on evolutionary operations and crossover to progressively refine architectures. This paradigm inevitably necessitates the instantiation, training, and subsequent evaluation of each generated model to ascertain its performance, a process that is notoriously resource-intensive. The iterative cycle of generating a population of architectures, training them for even a few epochs, and measuring their fitness creates a significant computational bottleneck, rendering the search process both time-consuming and expensive. Consequently, the practical application of such methods is limited, particularly in scenarios demanding efficient and lightweight architecture discovery.

Figure 16: zero-cost proxy1 discovered by APD in the NAS-Bench-201.

```python
import torch
import torch.nn as nn

def proxy1(model, inputs, targets):
    bn_ranks = []
    ratios = []
    hooks = []

    def bn_hook(module, inp, out):
        if isinstance(out, torch.Tensor):
            B, C, H, W = out.shape
            mat = out.view(B, C, -1).permute(0, 2, 1).reshape(-1, C)
            frob_norm = torch.linalg.matrix_norm(mat, ord='fro')**2
            spec_norm = torch.linalg.matrix_norm(mat, ord=2)**2
            stable_rank = frob_norm / (spec_norm + 1e-6)
            bn_ranks.append(stable_rank.mean())

    for layer in model.modules():
        if isinstance(layer, nn.BatchNorm2d):
            hooks.append(layer.register_forward_hook(bn_hook))
        elif isinstance(layer, nn.Conv2d):
            weights = layer.weight
            l1_norm = weights.abs().sum(dim=(1,2,3)).mean()
            l2_norm = weights.norm(p=2, dim=(1,2,3)).mean()
            ratios.append((l1_norm / l2_norm).item())

    with torch.no_grad():
        model(inputs)

    for hook in hooks:
        hook.remove()

    bn_sum = torch.stack(bn_ranks).sum().item() if bn_ranks else 0.0
    ratio_sum = sum(ratios) if ratios else 0.0

    return bn_sum * ratio_sum
```

Figure 17: zero-cost proxy2 discovered by APD in the NAS-Bench-201.

```python
import torch
import torch.nn as nn

def proxy2(model, inputs, targets):
    ratios = []
    spatial_stds = []

    activations = []
    def hook_fn(module, input, output):
        activations.append((module.weight.detach(), output.detach()))

    hooks = []
    for layer in model.modules():
        if isinstance(layer, nn.Conv2d):
            hooks.append(layer.register_forward_hook(hook_fn))

    with torch.no_grad():
        model(inputs)

    for hook in hooks:
        hook.remove()

    for weight, act in activations:
        weight_norm = torch.norm(weight, p='fro')
        act_norm = torch.norm(act, p='fro')
        if act_norm != 0:
            ratios.append((weight_norm / act_norm).item())

        spatial_std = act.std(dim=1, keepdim=True)
        spatial_stds.append(spatial_std.mean().item())

    avg_ratio = sum(ratios) / len(ratios) if ratios else 0.0
    avg_std = sum(spatial_stds) / len(spatial_stds) if spatial_stds
       else 0.0
    return -2 * (avg_ratio * avg_std) / (avg_ratio + avg_std + 1e-10)
```

Figure 18: zero-cost proxy3 discovered by APD in the NAS-Bench-201.

```
import torch
import torch.nn as nn

def proxy3(model, inputs, targets):
    activations = []

    def hook_cnn(module, input, output):
        activations.append(output.detach().flatten(2))

    hooks = []
    for layer in model.modules():
        if isinstance(layer, nn.Conv2d):
            hooks.append(layer.register_forward_hook(hook_cnn))

    with torch.no_grad():
        _ = model(inputs)

    for h in hooks:
        h.remove()

    scores = []
    for act in activations:
        act = act - act.mean(dim=-1, keepdim=True)
        channel_mean = act.abs().mean(dim=(0, 2))
        if channel_mean.mean() > 1e-6:
            cv = channel_mean.std() / channel_mean.mean()
            scores.append(cv.item())

    return -sum(scores) / len(scores) if scores else 0.0
```

Figure 19: zero-cost proxy1 discovered by APD in the TransNAS-Bench-101.

```
import torch
import torch.nn.functional as F

def proxy1(model, inputs, targets):
    inputs.requires_grad_(True)

    with torch.enable_grad():
        output = model(inputs)
        loss = F.cross_entropy(output, targets)
        grad_clean = torch.autograd.grad(loss, inputs)[0]

        output = model(inputs + 0.01)
        loss = F.cross_entropy(output, targets)
        grad_noisy = torch.autograd.grad(loss, inputs)[0]

    inputs.requires_grad_(False)
    cos_sim = F.cosine_similarity(grad_clean.flatten(), grad_noisy.
        flatten(), dim=0)
    return cos_sim.cpu().item()
    return score.cpu()
```

Figure 20: zero-cost proxy2 discovered by APD in the TransNAS-Bench-101.

```
import torch

def proxy2(model, inputs, targets):
    with torch.no_grad():
        clean_output = model(inputs)
        scaled_inputs = inputs * 1.01  # Small fixed scaling
        scaled_output = model(scaled_inputs)

    logit_diff = torch.norm(clean_output - scaled_output, p=2, dim=1)
        .mean()
    return logit_diff.cpu().item()
```

Figure 21: zero-cost proxy3 discovered by APD in the TransNAS-Bench-101.

```
import torch
import torch.nn.functional as F

def proxy3(model, inputs, targets):
    with torch.no_grad():
        clean_output = model(inputs)
        noise = torch.zeros_like(inputs)
        for i in range(inputs.shape[2]):
            for j in range(inputs.shape[3]):
                noise[:, :, i, j] = 0.01 * ((i + j) % 2 * 2 - 1)
        noisy_output = model(inputs + noise)

    clean_probs = F.softmax(clean_output, dim=1)
    noisy_probs = F.softmax(noisy_output, dim=1)

    kl_div = F.kl_div(clean_probs.log(), noisy_probs, reduction='
        batchmean')
    return kl_div.cpu().item()
    return score.cpu()
```

Figure 22: zero-cost proxy1 discovered by APD in the AutoFormer.

```
import torch
import torch.nn.functional as F

def heuristic_5(model, inputs, targets, loss_fn):
    with torch.no_grad():
        clean_output = model(inputs)
        noise_levels = [0.01, 0.05, 0.1]

        kl_values = []
        clean_probs = F.softmax(clean_output, dim=1)

        for level in noise_levels:
            noise = torch.randn_like(inputs) * level
            noisy_output = model(inputs + noise)
            noisy_probs = F.softmax(noisy_output, dim=1)
            kl_div = F.kl_div(clean_probs.log(), noisy_probs,
                reduction='batchmean')
            kl_values.append(kl_div)

        score = torch.prod(torch.stack(kl_values)) ** (1/len(
            kl_values))
    return score.cpu().item()
```

Figure 23: zero-cost proxy2 discovered by APD in the AutoFormer.

```python
import torch
import torch.nn.functional as F

def proxy2(model, inputs, targets, loss_fn):
    with torch.no_grad():
        # Input perturbation component
        noise = torch.randn_like(inputs) * 0.01
        perturbed_inputs = inputs + noise
        original_outputs = model(inputs)
        perturbed_outputs = model(perturbed_inputs)
        diff = torch.norm(original_outputs - perturbed_outputs, p=2,
            dim=1).mean()

        # KL divergence component
        original_softmax = original_outputs.softmax(dim=1)
        perturbed_softmax = perturbed_outputs.softmax(dim=1)
        kl_div = F.kl_div(original_softmax.log(), perturbed_softmax,
            reduction='batchmean')

    return (diff + kl_div).cpu().item()
```

Figure 24: zero-cost proxy3 discovered by APD in the AutoFormer.

```python
import torch

def proxy2(model, inputs, targets):
    with torch.no_grad():
        clean_output = model(inputs)
        scaled_inputs = inputs * 1.01  # Small fixed scaling
        scaled_output = model(scaled_inputs)

    logit_diff = torch.norm(clean_output - scaled_output, p=2, dim=1)
        .mean()
    return logit_diff.cpu().item()
```

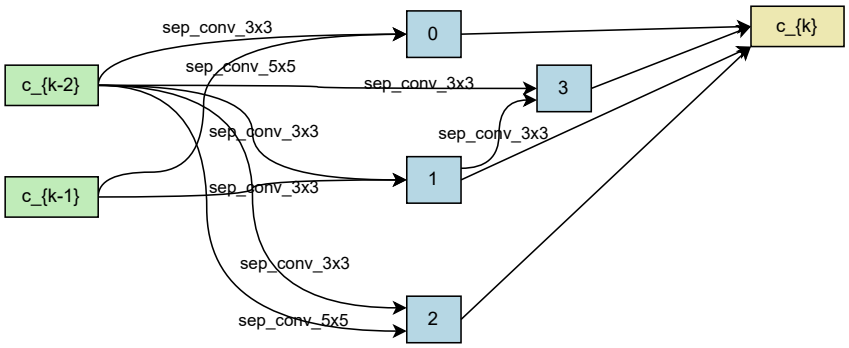

Figure 25: Normal cell searched by APD.

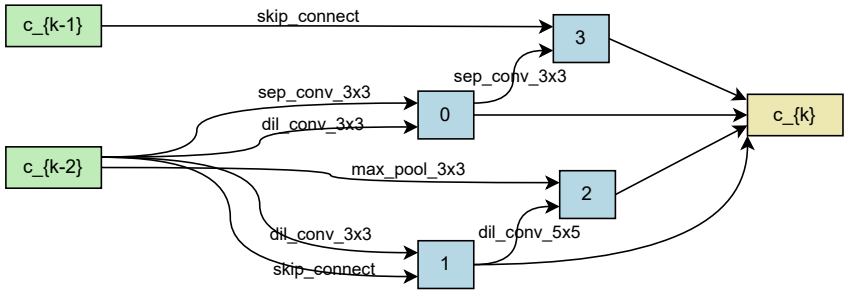

Figure 26: Reduction cell searched by APD.

Figure 27: Optimal structure found in the DARTS search space by APD.

```
Genotype(normal=[('sep_conv_3x3', 0), ('sep_conv_5x5', 1),
('sep_conv_3x3', 0), ('sep_conv_3x3', 1),
('sep_conv_5x5', 0), ('sep_conv_5x5', 0),
('sep_conv_3x3', 3), ('sep_conv_3x3', 0)], normal_concat=range(2, 6),
reduce=[('sep_conv_3x3', 0), ('dil_conv_3x3', 0),
('dil_conv_3x3', 0), ('skip_connect', 0),
('max_pool_3x3', 0), ('dil_conv_5x5', 3),
('sep_conv_3x3', 2), ('skip_connect', 1)], reduce_concat=range(2, 6))
```

Figure 28: Subnet discovered in the AutoFormer tiny search space by APD.

```
RETRAIN:
  MLP_RATIO:
  - 4
  - 3.5
  - 3.5
  - 3.5
  - 3.5
  - 4
  - 4
  - 4
  - 4
  - 3.5
  - 3.5
  - 3.5
  NUM_HEADS:
  - 4
  - 3
  - 4
  - 4
  - 4
  - 4
  - 4
  - 4
  - 3
  - 3
  - 3
  - 4
  DEPTH: 12
  EMBED_DIM: 240
```

Figure 29: Subnet discovered in the AutoFormer small search space by APD.

```
RETRAIN:
  MLP_RATIO:
    - 3.5
    - 3.0
    - 4.0
    - 4.0
    - 4.0
    - 3.0
    - 3.0
    - 3.0
    - 4.0
    - 4.0
    - 4.0
    - 3.0
    - 4.0
    - 3.0
  NUM_HEADS:
    - 7
    - 6
    - 7
    - 5
    - 7
    - 7
    - 6
    - 7
    - 7
    - 6
    - 5
    - 5
    - 7
    - 5
  DEPTH: 14
  EMBED_DIM: 448
```

Figure 30: Subnet discovered in the AutoFormer base search space by APD.

```
RETRAIN:
  MLP_RATIO:
    - 3.0
    - 3.0
    - 3.0
    - 4.0
    - 4.0
    - 3.5
    - 3.0
    - 4.0
    - 3.5
    - 3.0
    - 4.0
    - 3.0
    - 3.0
    - 4.0
    - 3.0
  NUM_HEADS:
    - 9
    - 10
    - 9
    - 10
    - 10
    - 9
    - 10
    - 9
    - 9
    - 10
    - 9
    - 9
    - 10
    - 9
    - 10
  DEPTH: 15
  EMBED_DIM: 576
```